

# SYNTHESIS OF METAL OXIDE NANOPARTICLES AND THEIR INHIBITORY ACTION FOR GLYCOSIDE HYDROLASES

## A DISSERTATION

*Submitted in partial fulfillment of the  
requirements for the award of the degree*

*of*

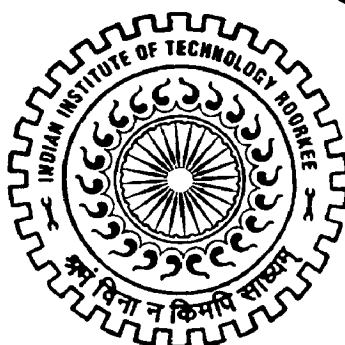
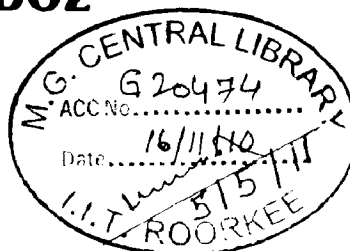
MASTER OF TECHNOLOGY

*in*

NANOTECHNOLOGY

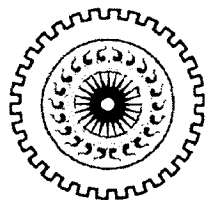
*By*

**SHAIK FIRDOZ**



CENTRE OF NANOTECHNOLOGY  
INDIAN INSTITUTE OF TECHNOLOGY ROORKEE  
ROORKEE-247 667 (INDIA)

JUNE, 2010



Indian Institute of Technology Roorkee  
Centre of Nanotechnology

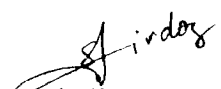
**CANDIDATE'S DECLARATION**

---

I hereby declare that the work which is being presented in the Dissertation entitled **“SYNTHESIS OF METAL OXIDE NANOPARTICLES AND THEIR INHIBITORY ACTION FOR GLYCOSIDE HYDROLASES”** in partial fulfillment of the requirements for the award of the degree of Masters of Technology submitted in the **Centre of Nanotechnology**, IIT Roorkee is an authentic record of my own work carried out during the period from November, 2009 to June, 2010 under the supervision and guidance of Prof. Anil Kumar.

The matter embodied in this project work has not been submitted for the award of any other degree.

Date 30/06/10

  
(Shaik Firdoz)

This is to certify that the above statement made by the candidate is correct to the best of my Knowledge.

  
(Dr. Anil Kumar)

Professor & Head  
Centre of Nanotechnology  
Indian Institute of Technology

## *Acknowledgements*

First of all I would like to pay my sincere gratitude to my beloved Prof. **Anil Kumar**, the founder of M.tech (Nanotechnology) course in IIT –Roorkee, without him , I may not get the chance to carry my dissertation work at IIT-Roorkee. I feel privilege and proud to work under his esteemed guidance. Secondly, I would like to thanks my best friend **Dara Nuthan** who has taken a very good decision in peak time and encouraged me to attend this interview and taken admission offer on behalf of me, without him, I may not get chance to join at IIT –Roorkee and carry this dissertation work. Thirdly, I would like to thanks Miss. **M. Jyothi** my colleague and friend at K.L.C.E who has supported and encouraged me to join at IITR. She has contributed to the best in her life to me. After paying sincere thanks to the above three eminent persons, I owe my gratitude to all those people who have made this dissertation possible and because of whom my graduate experience has been one that I will cherish forever.

My deepest gratitude is to my guide, **Prof. Anil Kumar**, who has given me a chance to work a patent dissertation work. I have been amazingly fortunate to have an advisor who gave me the freedom to explore on my own and at the same time the guidance to recover when my steps faltered and given a dissertation work. He taught me how to analyze the innovative things and to manage time for the best and expressed his valuable ideas and criticism on my dissertation work. He encouraged me to grow an independent thinker. I am grateful to him for holding me to a high research standard and enforcing strict validations for each research result, and thus teaching me how to do research. In spite of his busy schedule, he always spent his valuable time with me. His infectious enthusiasm and unlimited zeal have been major driving force through my M.Tech. I am deeply grateful to him for the long discussions that helped me sort out the technical details of my work. I am also thankful to him for encouraging the use of correct grammar and consistent notation in my writings and for carefully reading and commenting on countless revisions of this dissertation. His patience and support helped me overcome many crisis situations and finish this dissertation. I really wonder about his patience and hard working nature, I never saw him in angry mood with students and this creates a healthy environment to carry this dissertation work. I really thank for his valuable support during entire M.Tech course.

I would like to express my deep sense of gratitude to **Dr. Justin Thomas**, for his valuable support and suggestions during M.tech course.

This is a great opportunity to express my respect to **Dr. Jayaganathan** (co-ordinator M.Tech.) for his encouragement and practical advices. I am pleased to thank IISC Head for providing me instrumentation facility whenever I needed.

One of the most important persons who have been with me in every moment of my dissertation tenure is **Mr. Sudhir Kumar** and Bhupender my seniors. I would like to thank for their support. I specially thanks for Mr.Venkatesh, I always remember the fun I had with him in the lab.

I have been fortunate to come across very helpful, decent, noble and funny friend **Mr. U. Rajesh Kumar** without whom my life would be bleak. He helped me stay sane through my difficult, thorny, and problematic time. His support and care helped me overcome setbacks and stay focused on my study. I greatly value his friendship and I deeply appreciate his belief in me. I will forever remember the movies, tea, dinners, games I enjoyed with him.

Very special thanks to my child hood friends **Mr. Dara Nuthan**, Mr. Sai Naresh, Vishnu Prasad, Siva Lakshi and J.Bindhu madhavi for their support in my entire life. I would like to thanks Ranjit, Maheshwar reddy , sandeep and chalapathi my B.tech friends. In addition I would like to thanks Jaya aunty and his son Mr. Krishna Chaitanya (late) alias china ,who helped me a lot in my life and never forget his memorable friendship with him.

Where would I be without my family? Most importantly, none of this would have been possible without the love and patience of my family. My parents deserve special mention for their inseparable support and prayers. They continuously supporting me throughout my life and leaving me free in all my decisions. And finally I thank almighty GOD who plays all the game.

**Shaik Firdoz**



## Table of Contents

<i>Candidate's declaration</i>	i
<i>Acknowledgements</i>	ii
<i>Table of Contents</i>	iv
<i>List of figures</i>	vi
<i>Abstract</i>	viii
<i>List of publications</i>	ix
<b>Chapter 1 General Introduction</b>	
1.1 Nanotechnology	1
1.2 Classification of Nanomaterials	4
1.2.1 Carbonaceous Materials	4
1.2.2 Metallic Material	5
1.2.3 Composites/Hybrids	5
1.2.4 Ceramics	6
1.2.5 Semiconductors	6
1.3 Synthesis of Semiconductor Nanoparticles	7
1.3.1 Chemical methods	8
1.3.2 Metal Oxide	8
1.3.3 Titanium dioxide	8
1.3.4 Magnesium oxide	13
1.3.5 Iron oxide	13
1.3.6 Aim and Scope of the present work	14
<b>Chapter 2 Experimental Section</b>	
2.1 Materials	17
2.2 Equipment	17
2.2.1 Spectrophotometer	17
2.2.2 Spectrofluorophotometer	17
2.2.3 Infrared Spectrophotometer	18
2.2.4 Atomic force microscopy (AFM)	18
2.2.5 X-Ray diffractometer	19
2.2.6 Field emission scanning electron microscope (FE-SEM) coupled dispersive X-ray analysis (EDAX)	20

2.2.7	Single photon counting spectrometer	21
2.3	Methodology	21
2.3.1	Synthesis of thioglycerol capped ZnO nanoparticles (SP1)	21
2.3.2	Synthesis of Acarbose capped ZnO nanoparticles (SP2)	22
2.3.3	Characterization of TG-ZnO and Acarbose-ZnO nanoparticles	22
2.3.3.1	UV-Visible spectrometer	22
2.3.3.2	Spectrofluorophotometry	22
2.3.3	FT-IR Spectroscopy	22
2.3.3.4	Atomic force microscopy	23
2.3.3.5	X-Ray diffraction	23
2.3.3.6	Field emission scanning electron microscope (FESEM) coupled with energy dispersive X-ray analysis (EDAX)	23
2.3.3.7	Estimation of 1% Inhibition of nanoparticles with human salivary Amylase (HAS) for retardation of carbohydrate metabolism	23
<b>Chapter 3</b>	<b>Results and Discussion</b>	<b>25</b>
3.1	Electronic properties of SP1 and SP2 Nanosystems	25
3.2a	Emission Spectra of SP1 and SP2 Nanosystems	26
3.2b	Fluorescence Lifetime Decay curves	27
3.3	X-Ray Diffraction	29
3.4	FTIR Spectroscopy of samples	31
3.5	Morphology of nanosystems	36
3.6	Morphology and composition of Nanosystems	43
3.7	Inhibitory activity of SP1 and SP2 Nanosystems	47
3.8	Discussion	51
3.9	Conclusion	52
3.10	References	54

## *List of Figures*

<b>Figure 1</b>	Scale of Some Natural and Made objects	1
<b>Figure 1b</b>	Polymorphic forms of Titanium dioxide	9
<b>Figure 2</b>	Different forms of Zinc Oxide crystals	11
<b>Figure 3</b>	AFM	18
<b>Figure 4</b>	FESEM	20
<b>Figure 5</b>	UV-VIS absorption spectra of (A) SP1 Nanosystems (B) SP2 Nanosystems	26
<b>Figure 6A</b>	Emission spectra of (A) SP1 Nanosystems (B) SP2 Nanosystems	27
<b>Figure 6B</b>	Fluorescence lifetime decay of SP1, SP2, and SP3 Nanosystems	29
<b>Figure 7</b>	XRD pattern of (A) SPI (B) SP2 and (C) Bulk ZnO	31
<b>Figure 8</b>	IR spectra of TG	32
<b>Figure 8B</b>	IR spectra of E1	33
<b>Figure 8C</b>	IR spectra of D1	33
<b>Figure 8D</b>	IR spectra SP1 nanoparticles	34
<b>Figure 8E</b>	IR spectra of SP2 nanoparticles	34
<b>Figure 8F</b>	IR spectra of SP3 nanoparticle	35
<b>Figure 8G</b>	IR spectra of Bulk ZnO	35
<b>Figure 9A</b>	AFM of SP1 nanoparticles	37
<b>Figure 9B</b>	SP2 nanoparticles	39
<b>Figure 9C</b>	SP3 nanoparticles	41
<b>Figure 9D</b>	Only Enzyme (E1)	42
<b>Figure 10A</b>	FESEM of SP1 nanoparticles	43
<b>Figure 10B</b>	EDAX spectra SP1 nanoparticles	44
<b>Figure10.1A</b>	FESEM of SP2 nanoparticles	45
<b>Figure10.1B</b>	FESEM of SP2 nanoparticles	46
<b>Figure 10C</b>	FESEM and EDAX of acarbose	47
<b>Figure 11A</b>	Effect of [starch] on enzyme activity	49
<b>Figure 11B</b>	Effect of [SP1] on enzyme activity	49
<b>Figure 11C</b>	Effect of [SP2] on enzyme activity	50
<b>Figure 11D</b>	Effect of temperature on inhibitory action of nanoparticles on enzyme activity	50

<b>Figure 11E</b>	Effect of pH on inhibitory action of nanoparticles on enzyme activity	50
<b>Figure 11F</b>	Effect of [Drug] on enzyme activity	51

## *Abstract*

---

The present report describes the synthesis of water soluble biocompatible metal oxides nanoparticles in aqueous media. These particles have been characterized by using various spectroscopic and electron microscopy. Advanced tools like UV- Visible, emission, FT-IR, AFM and FESEM have been employed for their characterization. These particles depict the onset absorption about 320 nm and exhibit band gap emission at 377 nm. has been employed for their characterization. These features are fairly different to its bulk material and exhibit size quantization effect. By using Scherrer formula the particles size for the two studied nanosystems is observed to lie between to 10 – 12 nm. As synthesized nanosystems were examined to control the glycosidases activity in reference to develop a substitute for the standard drug having side effects. The inhibitory action of SP1 and SP2 nanoparticles with glycosidases was observed to be 61% and 72% respectively. Moreover, the inhibition activity of the studied nanosystems (SP1) was found to be very similar to that of standard drug being used for diabetes. The coating of these particles with drug demonstrated an enhancement in inhibition activity of the enzyme by about 30 %. To the best of our knowledge the first work describing the synthesis of drug capped nanoparticles and demonstrating the inhibition activity of enzyme both nanoparticles as well as drug coated nanoparticles.

## List of Publications

---

1. Submitted for **Patent rights** ( Review)
2. Presented a Paper and won the “**Best presentation Award**” on “**Metal oxide nanoparticles as a prospective Drug for Diabetes Mellitus type II and Obesity** ”  
**Anil Kumar, Shaik Firdoz** “the *International Conference on Advancement of Nanoscience and Nanotechnology (ICOANN-2010)*, Alagappa University, Karaikudi-630 003, Tamil Nadu.( March 1-3) ; NB-0P-08, P58.

# ***Chapter 1 General Introduction***

## ***1.1 Nanotechnology***


“Nanoscale” generally refers to objects lying in the range of 1–100 nm in either one or more dimensions. Nanotechnology is related to the fabrication of objects or devices whose features / functions are consequence of their nanoscale dimensions and / or organization. The unique properties of these materials *viz.* chemical, mechanical, electrical, photochemical, magnetic, electronic and thermal are not only different to their respective bulk analogues but are observed to exhibit both size and shape dependence. Nano range features inherit the nearly the function of larger bulk materials and depict a systemic variation in properties approaching to molecular dimensions [1].

Nature is a nanoarchitect consisting of large number of biological and other objects of nanodimensions. Some of these nano objects giving their size range are depicted in Fig. 1


Nanofabrication generally adopts two approaches: top down and bottom up. In top down approach one starts up with the respective bulk material and reduce its lateral dimensions leading to the production of nanostructures. The bottom up approach begins with atoms or molecules to build up nanostructures using a variety of physicochemical forces. For accomplishing these tasks both physical and chemical methods have been employed. Physical methods are commonly used for the fabrication of nanostructures using top down strategy such as photolithography, chemical vapour deposition, physical vapour deposition, micro contact printing and milling or attrition. Wet chemical methods are generally employed to synthesize nanostructures using bottom up approach such as hydrothermal, precipitation, oxidation, reduction, photochemical, radiation chemical and sol-gel.

## Scale of Some Natural and Man Made Objects

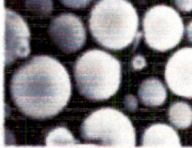
**Natural**




Dust mite  
↔  
200 μm



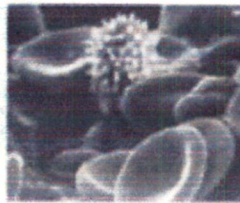
Ant  
~ 5 mm




Fly ash  
~ 10-20 μm



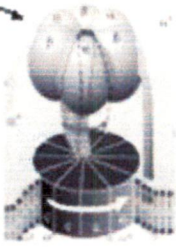
Human hair  
~ 60-120 μm wide



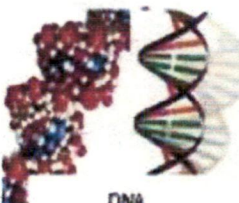
Red blood cells  
with white cell  
~ 2-5 μm



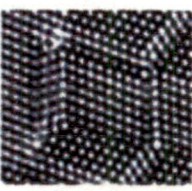
~ 10 nm diameter



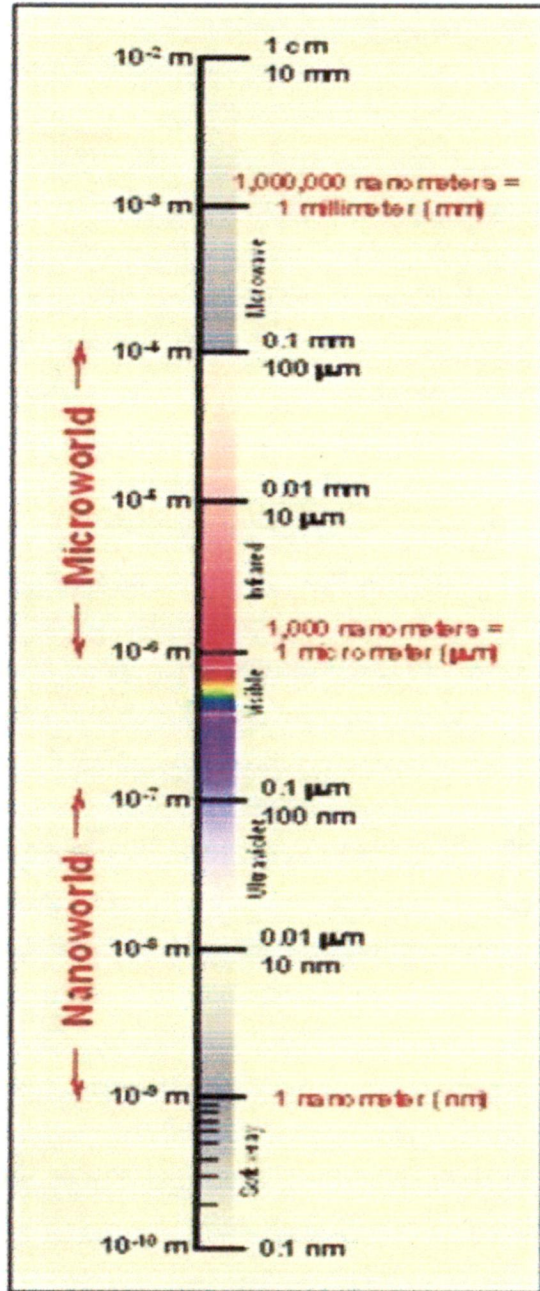
ATP synthase



DNA  
~ 2-12 nm diameter



Atoms of silicon  
spacing ~ tenths of nm





# Manmade

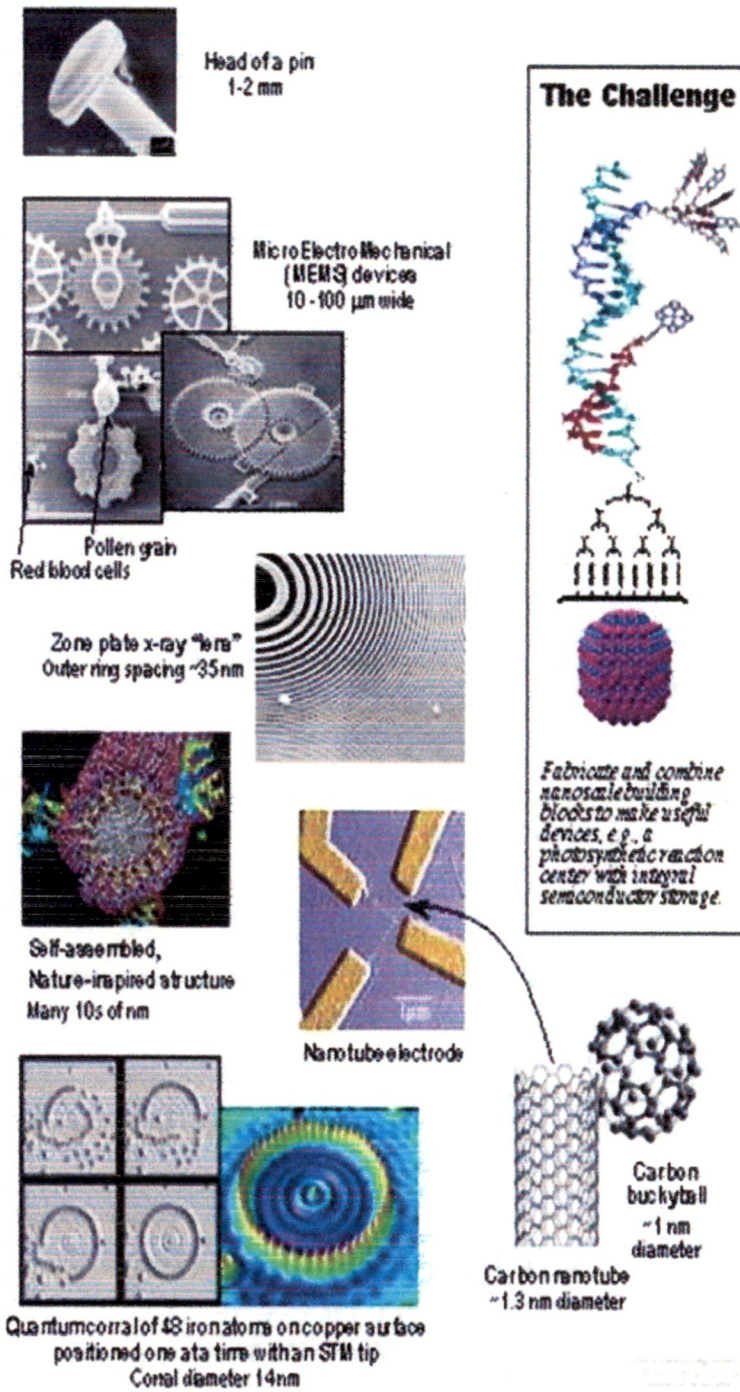


Fig.1: Taken from [http://www.nano.gov/html/facts/The\\_scale\\_of\\_things.html](http://www.nano.gov/html/facts/The_scale_of_things.html).

The conventional top-down processes hardly allow the production of the smaller objects of <100 nm, whereas the limits of regular bottom – up processes are in the range of about 1-10 nm.

## 1.2 Classification of Nanomaterials

Nanomaterials are mainly classified into different types based on dimensions and phase composition [2]. The main classes of nanoscale materials are summarised below

Dimension	Examples
Zero or three dimensions (< 100nm )	Particles, quantum dots, hollow spheres.

Phase composition	Examples
Single-phase solids	Crystalline, amorphous particles and layers.
Multi-phase solids	Matrix composites and coated particles.
Multi-phase system	Colloids, aerogels and ferrofluids.
Two dimensions (< 100 nm )	Tubes, fibres, wires and platelets.
One dimension (< 100 nm )	Films, coatings and multilayers.

Just like the bulk materials, nanomaterials can be classified as carbonaceous, metals and their alloys, semiconductors, nanohybrids, and ceramics.

### 1.2.1 Carbonaceous Materials

These nanomaterials are composed mostly allotropes of carbon, commonly taking a variety of shapes, form of a hollow spheres, ellipsoids, or tubes. Spherical and ellipsoidal carbon nanomaterials are referred to as fullerenes, while cylindrical ones are called

nanotubes. These particles have many potential applications as regard to uniformity of improved films and coatings, stronger as well as lighter materials, and usage as nanowires, computer chips and information storage in electronics. Dendrimers are nearly perfect monodisperse (basically meaning of a consistent size and form) macromolecules with a regular and highly branched three-dimensional architecture [3].

### ***1.2.2 Metallic Materials***

Metal is an element, compound, or alloy characterized by high electrical conductivity. Some of these materials at nanolevel viz. Rh, Pd, Ir, Pt, Au, Ag and Cu display characteristics optical, electronic, catalytic and conducting properties. A change in size and shape has been observed not only to bring a change in their properties but could also make them to behave as non-metallic [4].

### ***1.2.3 Composites / Hybrids***

Composite materials are engineered materials made from two or more constituent materials with significantly different physical or chemical properties, which remain separate and distinct on a macroscopic level within the finished structure. A nanocomposite is a multiphase solid material where one of the phases has one, two or three dimensions of less than 100 nm or structures having nano-scale repeat distances between the different phases that make up the material [4]. The mechanical, electrical, thermal, optical, electrochemical, catalytic properties of the nanocomposite(s) are markedly at variance from that of the parents components.

On the other hand hybrid materials as an intentional combination of two or more materials, complimenting each other to display super-functions / new functions differing to

nanotubes. These particles have many potential applications as regard to uniformity of improved films and coatings, stronger as well as lighter materials, and usage as nanowires, computer chips and information storage in electronics. Dendrimers are nearly perfect monodisperse (basically meaning of a consistent size and form) macromolecules with a regular and highly branched three-dimensional architecture [3].

### ***1.2.2 Metallic Materials***

Metal is an element, compound, or alloy characterized by high electrical conductivity. Some of these materials at nanolevel viz. Rh, Pd, Ir, Pt, Au, Ag and Cu display characteristics optical, electronic, catalytic and conducting properties. A change in size and shape has been observed not only to bring a change in their properties but could also make them to behave as non-metallic [4].

### ***1.2.3 Composites / Hybrids***

Composite materials are engineered materials made from two or more constituent materials with significantly different physical or chemical properties, which remain separate and distinct on a macroscopic level within the finished structure. A nanocomposite is a multiphase solid material where one of the phases has one, two or three dimensions of less than 100 nm or structures having nano-scale repeat distances between the different phases that make up the material [4]. The mechanical, electrical, thermal, optical, electrochemical, catalytic properties of the nanocomposite(s) are markedly at variance from that of the parents components.

On the other hand hybrid materials as an intentional combination of two or more materials, complimenting each other to display super-functions / new functions differing to

those of component materials [6]. Nanohybrids are defined as atomic or molecular level mixture of different materials bound mainly through supramolecular forces.

### ***1.2.4 Ceramics:***

A ceramic is an inorganic, non-metallic solid prepared by the action of heat and subsequent cooling. Ceramic materials may have a crystalline or partly crystalline structure, or may be amorphous (e.g., a glass) [7]. Because most common ceramics are crystalline, the definition of ceramic is often restricted to inorganic crystalline materials, as opposed to the non-crystalline glasses. Nanoceramics are defined as novel bulk materials or coating with microstructural architecture, characterized by at least one of the ceramic phases having length scale between 1 and 100 nm.

The major drive for wider interest in nanoceramics and its composites has been the fact that one can potentially achieve better and some unusual material properties by manipulating length scale in the nano range. Therefore, better performance and newer application of the materials, for example, durable bone replacement materials using polymer–ceramic.

### ***1.2.5 Semiconductors***

A semiconductor is a material that has an electrical conductivity between that of a conductor and an insulator. Quantum dots (QDs) are the inorganic semiconductor nanocrystal whose sizes are smaller than the Bohr exciton radius and display size dependent optical properties [6-7]. The QDs can be manipulated to exhibit with increased efficiency, tailored optical and emission in wide wavelength range act as photostable dye unlike their organic analogues. For these characteristic features, quantum dots have replaced the organic dyes for biological sensing / bio and imaging application. The applications of QDs have been explored in various domains of science and technology, e.g., transistors, solar cells, LEDs, lasers and

agents for medical imaging [8]. By controlling the sizes of the QDs it has not only been possible to achieve in vivo imaging of different structures in a cell and in tissues but also it has been possible to image cellular interactions using multicolor QDs [9]. In addition, these materials are finding excellent applications in nanodiagnostics, targeted drug delivery, and photodynamic therapy. Among various semiconductor oxides ZnO, TiO<sub>2</sub> and Fe<sub>2</sub>O<sub>3</sub> are known to be present in natural system. These found to be the most promising because of being economically viable, non-toxic and for their wide applications.

### ***1.3 Synthesis of Semiconductor Nanoparticles***

A variety of the synthetic methods comprising both the physical and chemical approaches are being used for the preparation of semiconductor nanoparticles. Most of these methods produce polydispersed particles due to the fluctuations in growth conditions such as gas flow, growth temperature and dispersion of precursors. Therefore, efforts to develop synthetic processes for the production of mono- dispersed particles still remains a challenging task for the effective usage of these materials in making of photonic and electronic devices [10].

**Physical methods:** Several physical methods namely, molecular beam epitaxy (MBE), thermal evaporation, metal-organic chemical vapour deposition (MOCVD), sputtering and laser ablation have been used for the preparation of semiconductor nanoparticles from desired material source [11-17]. These nanoparticles are generally obtained in the form of solid powder or thin films. The major drawback of these methods had been that the nanocrystals thus produced remain attached to the matrix, which limits their practical applications for making devices.

### ***1.3.1 Chemical methods***

The chemical methods include solvothermal [18, 19], sonochemical [20], microwave [21, 22], sol-gel [23], photochemical [24, 25] and radiolysis [26]. Synthesis of colloids using wet chemistry has provided an interesting methodology to grow different nanostructures in solution using bottom up approach, which provides greater flexibility and reproducibility. Moreover, it offers convenient means for nanofabrication of integrated materials for applications in the area of catalysis, LEDs, solar cells, biology, lasers, photodetectors, sensors, biology and medicine.

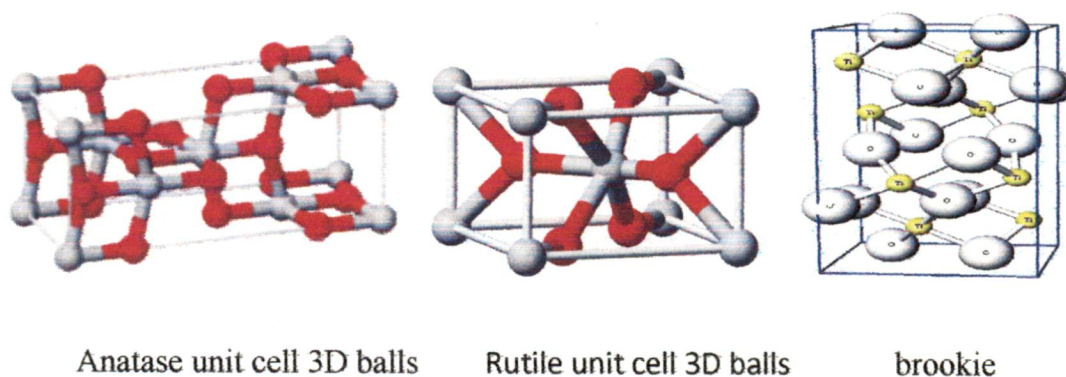
Synthesis of various II-VI [27, 28] and III-V [29] semiconductor nanoparticles have been carried out using wet methods. It specifically includes the synthesis of sulphides: CdS [30], ZnS [31-33]; oxides: ZnO [34], TiO<sub>2</sub> [35], MgO and Fe<sub>2</sub>O<sub>3</sub> [36].

### ***1.3.2 Metal Oxides***

Among various natural oxides, titanium dioxide, zinc oxide and iron oxides have been very popular. Some of these oxides like TiO<sub>2</sub> and ZnO have been employed both on ceramics and semiconducting materials.

### ***1.3.3 Titanium dioxide (TiO<sub>2</sub>)***

Titania is among one of the most widely studied ceramic oxides due to its unique optical and electrical properties. It has found a wide range of utility as photocatalyst(s), ceramic membrane, and in paints, solar cells, nonlinear optics, laser, diodes, varistors, gas sensor and humidity sensors [37]. Titania occurs in three polymorphic forms namely, rutile, anatase and brookite.



([www3.interscience.wiley.com/journal/120698277/articletext?DOI=10..](http://www3.interscience.wiley.com/journal/120698277/articletext?DOI=10..))

**Figure 1b : Polymorphic forms of Titanium dioxide**

Matijevi et al [38] prepared of Ti (IV) ion at 98 °C in highly acidic media in the presence of sulfate ion. The anatase phase was also found to be involved with increasing sulfate concentration. The mean size was on the order of a few micrometers. Bowen [39] and Ogihara *et al.* [40] prepared uniform amorphous titania spheres on the order of sub micrometers by the hydrolysis of titanium tetraethoxide in ethanol or a mixed solvent of acetonitrile and octanol in sol-gel systems.

Among other metal oxides, ZnO has been widely used in the area of light emitting diodes, gas sensors, optoelectronic, and circuitary due to its unique optical, piezoelectric, semiconducting, magnetic and thermal properties. Besides, it is extensively used as a UV blocker in skin protection gels and creams because of its non-toxic nature and biocompatibility [41].

Zinc oxide is an inorganic amphoteric oxide . It usually appears as a white powder, nearly insoluble in water and occurs as white powder known as zinc white or as the mineral zincite. The high exciton binding energy (60 meV) in ZnO crystal can ensure efficient excitonic emission at room temperature and room temperature ultraviolet (UV) luminescence

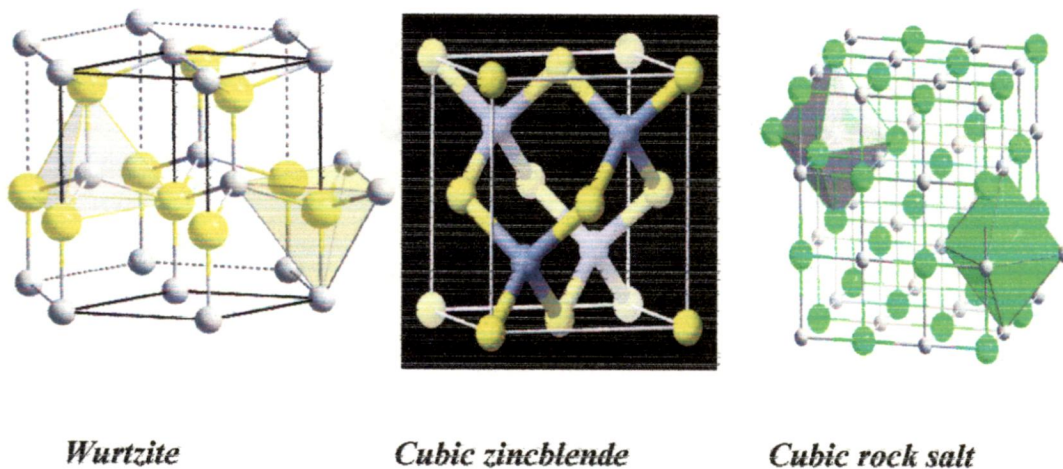


has been reported in disordered nanoparticles and thin films. ZnO is transparent to visible light and can be made highly conductive by doping.

Zinc oxide crystallizes in three forms: hexagonal wurtzite, cubic zincblende, and the rarely observed cubic rocksalt). The wurtzite structure is most stable at ambient conditions and thus most common. The zincblende form can be stabilized by growing ZnO on substrates with cubic lattice structure. In both cases, the zinc and oxide centers are tetrahedral. The rocksalt (NaCl-type) structure is only observed at relatively high pressures about 10 GPA [42].

Hexagonal and zincblende polymorphs have no inversion symmetry (reflection of a crystal relatively any given point does not transform it into itself). This and other lattice symmetry properties result in piezoelectricity of the hexagonal and zincblende ZnO, and in pyroelectricity of hexagonal ZnO.

The lattice constants for hexagonal wurtzite form are  $a = 3.25 \text{ \AA}$  and  $c = 5.2 \text{ \AA}$ ; their ratio  $c/a \sim 1.60$  is close to the ideal value for hexagonal cell  $c/a = 1.633$  [25]. Due to the polar Zn-O bonds, zinc and oxygen planes bear electric charge (positive and negative, respectively). Therefore, to maintain electrical neutrality, those planes reconstruct at atomic level in most relative materials, but not in ZnO - its surfaces are atomically flat, stable and exhibit no reconstruction. This anomaly of ZnO is not fully explained yet [43].



*Wurtzite*

*Cubic zincblende*

*Cubic rock salt*

**Fig.2 Different forms of Zinc Oxide crystals**

*(Taken from [ieeexplore.ieee.org/iel5/4816218/4831622/04831672.pdf?arnumber](http://ieeexplore.ieee.org/iel5/4816218/4831622/04831672.pdf?arnumber)).*

ZnO has been synthesized in different morphologies viz. nanoparticles, nanowires, nanosheets, nanorings, by using a variety methods such as hydrolysis, pyrolysis, precipitation and hydrothermal methods [44-49]. Zhang *et al.* reported a simple solution method for the synthesis of ZnO with well – defined controlled morphologies viz. flowerlike, snowflake-like, prismatic, prickly sphere-like and rod like by decomposing  $\text{Zn}(\text{OH})_4^{2-}$  or  $\text{Zn}(\text{NH}_3)^{2+}$  precursors under varied experimental conditions. These nanostructures exhibit photoluminescence in different wavelength range (385 - 510 nm) with other morphology dependent features. Tian *et al.* [50] synthesized large array of extended and oriented helical nanorods and columns of ZnO using citrate ions as controlling agent for the growth of these nanostructures.

Hexagonal prismatic ZnO whiskers with significantly uniform length and width have been prepared by the reduction and followed by oxidation of ZnS powder at 1300 °C [42]. These whiskers display both sharp and broad emission band at 388 nm and 515 nm,

respectively. Kumari et al. synthesized pencil-head-like (PHL) microprisms ZnO by a hydrothermal route using a zinc plate as a source and substrate [51].

Lately, sonochemical synthesis of Mg doped ZnO Nanoparticles depicting strong visible luminescence (~ 60%), has been reported [52]. An increase in the molar ratio of Mg/ZnO from 0 to 1.6 increases the band gap from 3.4 eV to 3.8 eV, which is associated with a blue shift in the emission maximum. An alkoxide based synthesis of spherical ZnO nanocrystal in wurtzite phase involving diethylzinc precursor in tert-butyl alcohol, ethanol and water mixture has been reported [53]. These particles were characterized by high surface area (110-120 m<sup>2</sup>/g), 2-5 nm crystalline size and unprecedented high reactivity. The growth of zinc oxide crystals can be limited by using various capping agents. Wu et al. were synthesized nano-crystalline ZnO particles using alcoholic solutions of zinc acetate dihydrate through a colloidal process by using of five types of capping agents: 3-aminopropyl trimethoxysilane (Am), tetraethyl orthosilicate (TEOS), mercaptosuccinic acid (Ms), 3-mercaptopropyl trimethoxysilane (Mp) and polyvinylpyrrolidone (Pv) were added at the first ZnO precipitation time (1st PPT) to limit the particle growth. The first three capping agents effectively capped the ZnO nanoparticles and limited the growth of the particles, while the last two capping agents caused agglomeration or larger clusters in the solutions. Singh et al. synthesized zinc oxide nanoparticles using the chemical method in alcohol base and studied the effect of size with different capping agents like triethanolamine (TEA), oleic acid and thioglycerol [52]. In this study thioglycerol has found to be effective capping agent and the size of particles found to be ~3 nm. Rajendran et al. [54] studied the development of antimicrobial cotton fabrics using Zinc oxide nanoparticles. The ZnO Nanoparticles were prepared by wet chemical method and were directly applied on to the 100% cotton woven fabric using pad-dry-cure method the usage of ZnO for the production of antimicrobial

textiles. Similarly, the ZnO nanoparticles enhanced antibacterial activity of ciprofloxacin against *Staphylococcus aureus* and *Escherichia coli*. Khan et al. [55] studied the usage of ZnO nanoparticles for cholesterol sensor.

The above literature survey reveals a variety of approaches for the synthesis of ZnO and its applications in diverse fields. These studies though lack its preparation by using the biocompatible capping agents in aqueous medium, which might find its usage as a prospective drug.

### ***1.3.4 Magnesium oxide (MgO)***

Magnesium oxide has found diverse applications in the areas of electronics, catalysts, toxic waste treatment, cosmetics, and paint in refractory materials [56].

### ***1.3.5 Iron Oxides***

Superparamagnetic iron oxide nanoparticles (SPION) with appropriate surface chemistry have been widely used experimentally for numerous *in vivo* applications such as magnetic resonance imaging contrast enhancement, tissue repair, immunoassay, detoxification of biological fluids, hyperthermia, drug delivery and in cell separation, etc. All these biomedical and bioengineering applications require that these nanoparticles have high magnetization values and size smaller than 100 nm with overall narrow particle size distribution, so that the particles have uniform physical and chemical properties. In addition, these applications need special surface coating of the magnetic particles, which has to be not only non-toxic and biocompatible but also allow a targetable delivery with particle localization in a specific area. Gupta and Gupta [57] have discussed the synthetic chemistry, fluid stabilization and surface modification of superparamagnetic iron oxide nanoparticles along with their usage for above biomedical applications. Michael and Ferrier [58] have discussed a complete characterization

of a configuration about their binding with biomolecules that is easy to use, in which a permanent magnet provides a fairly uniform gradient over a relatively large area.

### ***1.3.6 Aim and Scope of the present work***

The general objective of this thesis is to synthesize metal oxide nanoparticles in aqueous medium for their application as prospective drug in treatment of diabetes and obesity.

Diabetes is defined as a group of diseases characterized by high levels of blood glucose resulting from defects in insulin production, insulin action, or both. There are three main types of diabetes: type I results from the body's failure to produce insulin, and requires the person to inject insulin externally. Type II diabetes (non insulin-dependent diabetes) results from insulin resistance, a condition in which cells fail to use insulin properly, sometimes combined with an absolute insulin deficiency. Gestational diabetes generally occurs in pregnant women, who never had diabetes before, but gets a high blood glucose level during pregnancy. It may proceed eventually to develop of type II diabetes.

Among these the incidence of type II diabetes is increasing at an alarming rate. Diabetes alone ranks as the third most prevalent disease around the world. The numbers of worldwide sufferers are expected to rise from the present 177 million to 300 million individuals by 2030 [59]. This chronic disease takes a high toll in terms of human health and the cost of health care. Beyond the reduced quality of life and life expectancy, nearly 40% people afflicted with diabetes also likely to develop long-term complications such as hypertension, hyperlipidemia, cardiovascular disease, cancer, stroke, kidney failure and blindness [60]. A significant risk factor for the development of diabetes is obesity, which in itself has become a serious health issue [61]. Human  $\alpha$ -amylases of both salivary (HSA) and pancreatic origins (HPA) have been thoroughly studied from the viewpoint of clinical

chemistry because they are important as indicators in evaluating diseases of pancreas and salivary glands [62]. A number of studies have been made for their biochemical and structural characterization [63].

HSA is a key enzyme in the digestive system and catalyzes the initial step in the hydrolysis of starch, which is a principal source of glucose in the diet. Detailed structural and mechanistic studies have been performed on HSA, including analyses of HSA-inhibitor binary complexes [64]. It has been previously demonstrated that the activity of HSA in the digestive system correlates to post-prandial glucose levels, the control of which is an important factor in diabetes and obesity [65]. Modulation of HSA activity through the therapeutic use of inhibitors would, therefore, be of considerable medical relevance in the treatment of these debilitating diseases. Although two HSA inhibitors, acarbose (Precose™ or Glucobay™) and miglitol (Glyset™) are in current medical use but their effectiveness is limited by deleterious side effects related to dosage(s) to be administered [66]. New and more effective human drugs that can target HSA specifically, and can operate with relatively longer-term effects and lower systemic availability would be among valuable tools to combat the rapidly increasing incidences of these conditions. In this context many organic and inorganic materials have been explored as starch blockers [67]. These agents inhibit  $\alpha$ -amylases, thereby, preventing dietary starches from being absorbed by the body via inhibiting breakdown of complex sugars to simpler ones and less sugar would be made available for assimilation, helping in controlling diabetes. In recent years nanotechnology has enabled to enhance several properties of materials including bioactivity. Although, metal oxide nanoparticles have been used so far in cosmetics, dye industry, and in few domains of biomedicine only, but it has not been explored as an active drug.

In order to achieve this general objective, the aim of the present thesis is: To synthesize water soluble biocompatible nanoparticles in aqueous media and to examine its inhibition activity for the control of diabetes.

Keeping in view of the above literature survey, we report on synthesis and characterization of metal oxide nanoparticles using conventional techniques. It also discusses their potential as novel glycoside hydrolases inhibitors and compares its inhibition activity with standard drug, being used commonly for diabetes. To the best of our knowledge we have reported for the first time the synthesis of drug and thioglycerol matrix capped water soluble metal oxide nanoparticles and their usage as prospective active drug for type II diabetes

## Chapter 2 Experimental Section

### 2.1 Materials

Metal acetate [Loba]; NaOH, starch [Merck]; 1-thioglycerol, bulk material [Himedia], 3, 5-dinitrosalicylic acid (DNS), [Na-K-tartrate] [Sd-Fine]; glycoside hydrolases (Type IX-A, lyophilized powder, 1,000-3,000 units/mg protein) [Sigma]; standard drug is a gift from Jiang Bin, Hit, China and all other chemicals used were of analytical grade and were used without any further purification.

All experiments were carried out in double distilled water as these samples are very sensitive to impurities. For the preparation of double distilled water, single distilled water was transferred to an electrically heated five liter borosil glass distillation apparatus. Appropriate amounts of sodium hydroxide and potassium permanganate were added to this solution. Sodium hydroxide maintained the desired conductivity of the solution while  $\text{KMnO}_4$  oxidized the traces of organic impurities. All samples were freshly prepared before each study.

### 2.2 Equipment

#### 2.2.1 Spectrophotometer

The UV-Visible absorption spectra were recorded on Shimadzu UV-2100/s and Cary 5000.

#### 2.2.2 Spectrofluorophotometer

Steady-state emission spectra were on Shimadzu RF-5301 PC spectrofluorophotometer fitted with two monochromators, one each in excitation and



emission port, respectively. To block the undesired radiations suitable glass filters were also mounted in both excitation and emission ports to stop undesired radiations.

### 2.2.3 Infrared Spectrophotometer

IR Spectra were obtained on a Thermo Nicolet Nexus FTIR spectrophotometer in mid IR range in KBR medium. All spectra were recorded in transmission mode.

### 2.2.4 Atomic Force Microscopy (AFM)

The surface topographic analyses of the samples were performed on a NTEGRA (NTMDT) atomic force microscope. It has a built –in optical system which allows imaging of the scanning process with 1 $\mu$ m resolution. The resolutions in x-y and z directions are 0.1 to 1.0 nm and 0.01 nm, respectively.

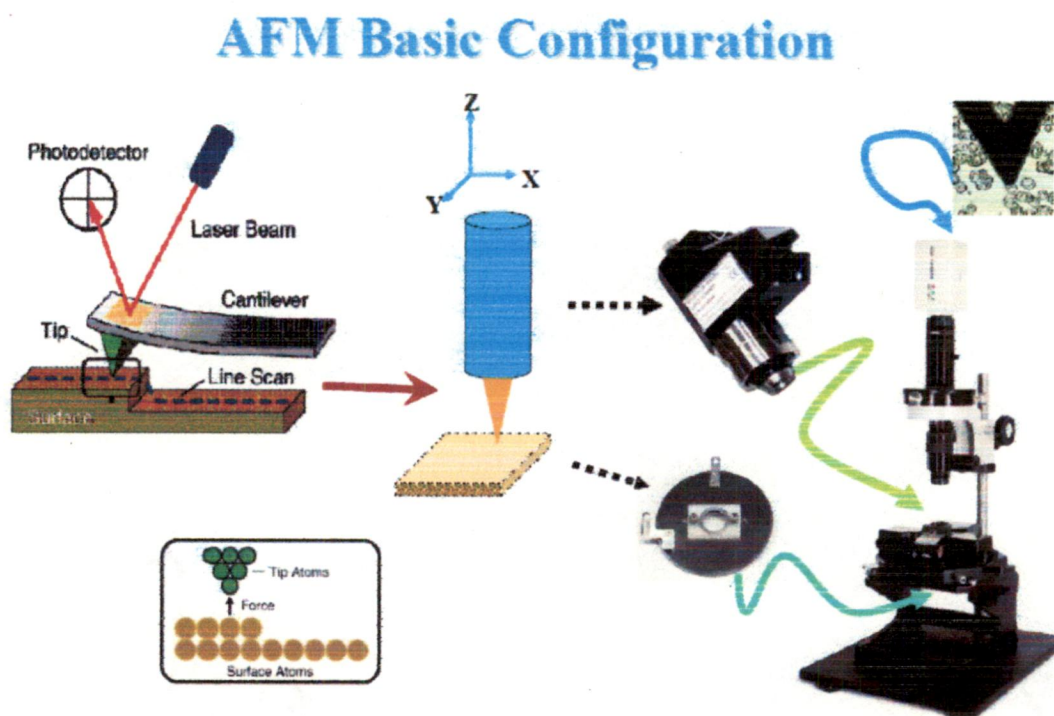


Fig.3 AFM (Taken from [www.agilent.com](http://www.agilent.com))

### **2.2.5 X-Ray Diffractometer**

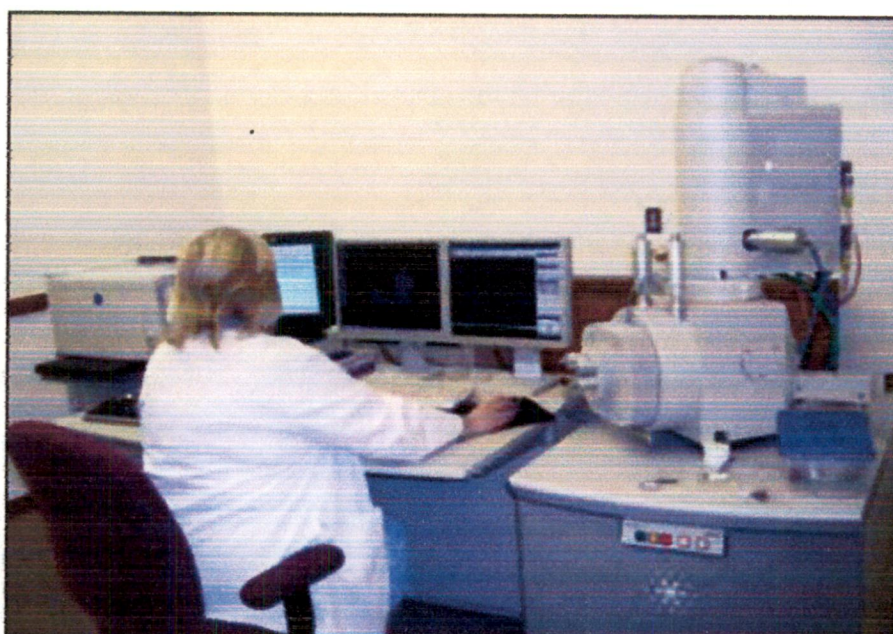
X-Ray diffraction patterns were recorded on a Philips DW 1140/90 X-ray diffractometer using Cu K $\alpha$  line (1.5418 Å) of the X-Ray source. X rays having wavelength similar to that of the size of the atom can be used to probe crystalline structure at the atomic level. Each crystalline solid has its unique characteristic X ray pattern, which may be used as a "fingerprint" for its identification. X ray crystallography may also be used to determine the packing of atoms in the crystalline state and to know about the inter atomic distance and angle of different planes. XRD being used extensively for the determination of the crystalline structure of nanocrystals [68]. A shape factor is used in x-ray diffraction and crystallography to correlate the size of sub-micrometre particles, or crystallites. In a solid, the broadening of a peak in diffraction pattern can be used to determine the size of nanoparticle by applying Scherrer equation,

$$(t = K \times \lambda / \beta \cos \theta)$$

where  $t$  is the average thickness of the particle,  $\lambda$  is the X-ray wavelength,  $\beta$  is the line broadening at half the maximum intensity in radians, and  $\theta$  is the Bragg angle, where  $K$  is the shape factor,  $\lambda$  is the x-ray wavelength, typically 1.54 Å,  $\beta$  is the line broadening at half the maximum intensity (FWHM) in radians, and  $\theta$  is the Bragg angle;  $\tau$  is the mean size of the ordered (crystalline) domains, which may be smaller or equal to the grain size. The dimensionless shape factor has a typical value of about 0.9, but varies with the actual shape of the crystallite. The Scherrer equation is limited to nano-scale particles. It is not applicable to grains larger than about 0.1  $\mu\text{m}$ , which precludes those observed in most metallographic and ceramographic microstructures.

### ***2.2.6 Field Emission Scanning Electron microscope (FESEM) coupled with Energy dispersive X- ray Analysis (EDAX)***

The surface morphology of the samples were analyzed by FEI-QUANTA 200 F field emission scanning electron microscope having maximum accelerating voltage of 40 kV. The elemental analyses of the synthesized materials were performed using EDAX accessory equipped with CCD camera.



**FESEM**

***Fig.4 FESEM***

*(Taken from [journals.cambridge.org/production/action/cjoGetFulltext?](http://journals.cambridge.org/production/action/cjoGetFulltext?))*

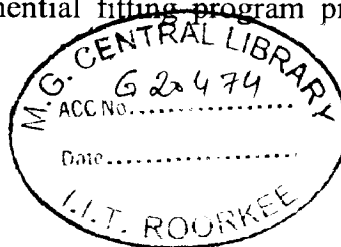
An electron microscope is employed to produce an electronically-magnified image of a specimen for finding its intricacies. In electron microscope (EM) a particle beam of electrons illuminates the specimen and create its magnified image. Unlike optical microscope in electron microscope and can achieve magnifications of up to 1,000,000X or

more, because the wavelength(s) about 100,000 times shorter compared to visible light radiation, whereas light microscopes are limited to 2000X magnification. Unlike the TEM, where electrons of the high voltage beam carry the image of the specimen, the electron beam of the Scanning Electron Microscope (SEM) produces images by probing the specimen with a focused electron beam that is scanned across a rectangular area of the specimen. At each point on the specimen the incident electron beam loses some energy, and that lost energy is converted into other forms, such as heat, emission of low-energy secondary electrons, light emission (cathode luminescence) or X-ray emission. The display of the SEM maps the varying intensity of any of these signals into the image in a position corresponding to the position of the beam on the specimen.

Since the SEM image relies on surface processes rather than transmission, it is able to image bulk samples up to many centimetres in size and has a great depth of field, and so can produce images that are good representations of the three-dimensional shape of the sample.

### ***2.2.7 Single Photon counting Spectrometer***

Fluorescence lifetime decay curves were recorded on a Horiba Jobin Yvon-IBH 'FluoroCube Fluorescent Lifetime System' in time domain mode. The 295 nm Nano LED was used as pulsed excitation source working at 1 MHz repetition rate in reverse mode. The emitted photons were detected by Hamamatsu (R 3809 U) photomultiplier and thermoelectrically cooled TBX-04-D detector. Decay curves were analyzed by iterative reconvolution technique using multiexponential fitting program provided from IBH. Data analysis was carried out DAS 6.1 software.



## ***2.3. Methodology***

### ***2.3.1 Synthesis of Thioglycerol Capped Metal Oxide Nanoparticles (SP1)***



Synthesis of metal oxide nanoparticles was carried out by a precipitation method; Take 10 mL NaOH (0.05 M) and 0.1 mL of respective TG (0.05 M) in a beaker and then stirred for 30 min on magnetic stirrer. To this solution 10 mL metal acetate (0.04 M) solution was taken and added drop-by-drop while stirring. After nearly two hours stirring, a milky white solution obtained, which was precipitated using acetone and the solution was left overnight. Next day, the precipitate was washed with acetone and washing procedure was repeated five times to get rid of excess TG. This sample was dried under vacuum at 50 °C for about six hours.

### ***2. 3.2 Synthesis of Drug Capped Nanoparticles (SP2)***

Similarly, for the synthesis of acarbose capped nanoparticles, these particles were precipitated in the presence of acarbose. In this case the precipitate obtained was washed with water and washing procedure was repeated to get rid of excess acarbose.

### ***2.3.3 Characterization of SP1 and SP2 Nanoparticles***

#### ***2.3.3.1 UV – Visible Spectrophotometer***

The TG and acarbose coated metal oxide particles were dispersed in water by sonication. The electronic spectra of these samples were measured in a 5 mm quartz cuvette. All spectra were recorded at room temperature.

#### ***2.3.3.2 Spectrofluorophotometry***

The steady state emission fluorescence spectra of ZnO dispersed water samples were recorded in a 5 cm quartz cuvette.

#### ***2. 3.3.3 FT-IR Spectroscopy***

IR spectra were recorded in mid range (4000 – 500  $\text{cm}^{-1}$ ). Measurements were made by preparing thin films of solid sample in KBr medium by pressing it under hydraulic press.

#### ***2.3.3.4 Atomic Force microscopy***

Surface topography of nanostructures was analyzed with an atomic force microscope operating under semi- contact mode at room temperature. Samples for AFM analysis were prepared by applying a drop of the solution on to a glass plate and then drying it under vacuum at room temperature. Images were recorded both in 2D and 3D.

#### ***2.3.3.5 X-Ray Diffraction***

The X- ray diffraction patterns of solid samples were recorded by using Cu  $K\alpha$  line (1.5418  $\text{Å}$ ) of the X- ray source. The acceleration voltage was kept at 40 kV with 30 mA flux. For all samples the diffraction patterns were recorded in 2 theta ranges from 20 to 90° at scanning speed of 1°/ min.

#### ***2.3.3.6 Field Emission Scanning Electron Microscope***

For FESEM analysis, powdered samples were taken on a glass slide and it was put in sputtering chamber for coating of a thin layer of gold 50 s at 30 $\mu$ A current to make the sample conducting. The sample was scanned under 10, 15, and 20 keV accelerating voltage to record the surface morphology at different magnifications. The distribution of different elements present in the samples was analyzed by EDAX.

#### ***2.3.7 Estimation of % Inhibitory Action of Nanoparticles with Glycoside Hydrolases for Retardation of Carbohydrate Metabolism***

Take 4 ml starch solution (1%) in different test tubes containing varied concentration of nanoparticles (10 µg / mL to 50 µg / mL) followed by the addition of 1ml of enzyme to these test tubes. This sample was incubated for 15 min at room temperature. The enzyme reacts with the starch solution to give the glucose as product. The amount of glucose was estimated by dinitrosalicylic method. The OD of the complex between glucose and DNS reagent was monitored at 540 nm by UV spectrophotometer using controlling solution (with out inhibitor) as a reference Percentage inhibition was calculated using the following formula:

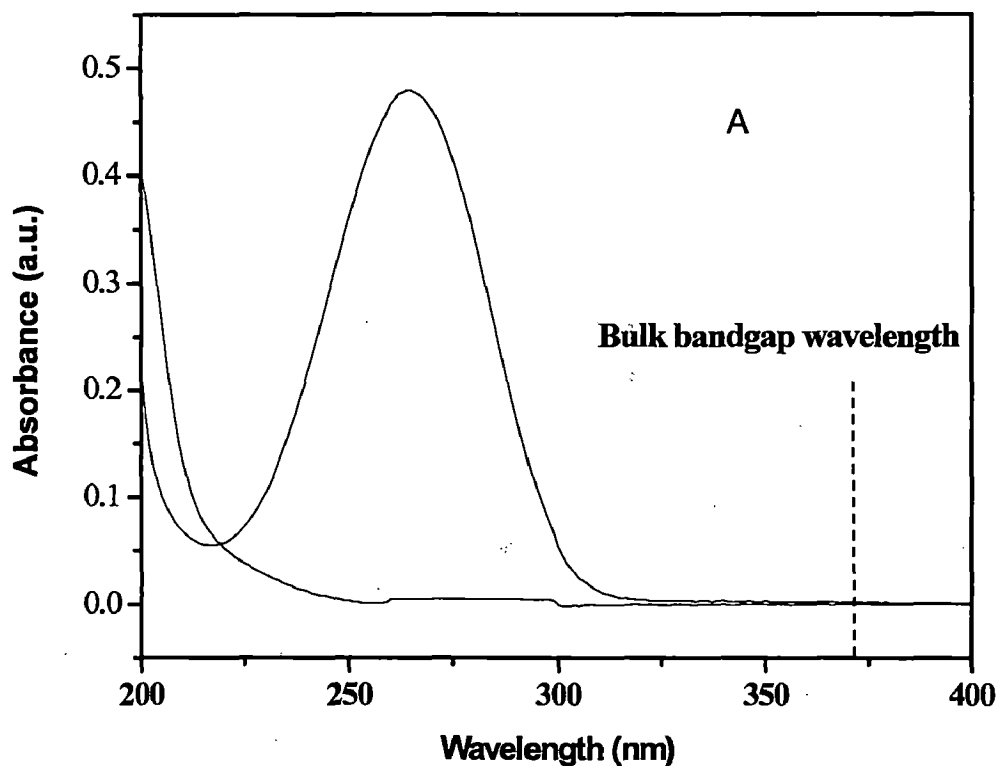
$$\% \text{ inhibition} = [\text{OD of control (A}_0) - \text{OD of test (A)} / \text{OD of control (A}_0)] * 100.$$

If the difference (OD of control – OD of test) was obtained as a positive number, it meant that the inhibition in amylase enzyme activity had occurred.

## Chapter 3: Results and Discussion

### 3.1 Electronic properties of SP1 and SP2 Nanosystems

The prepared nanopowders of SP1 and SP2 dispersed in water. Fig.5 presents its optical absorption spectrum along with the absorption blank of thioglycerol and drug. This spectrum shows an onset of absorption at 323 nm for SP1 and 320 nm (3.87 eV) for SP2 samples respectively, which is quite different to the band edge of the corresponding metal oxide bulk ( $E_g = 3.3$  eV) (shown as dotted line in Fig. 5) [69].



Besides, these samples exhibit prominent absorption peak (s) at 263 nm and 260 nm, which might have arisen due to their respective excitonic absorption. It may be mentioned that thioglycerol and drugs used as capping agent does not depict any absorption in this region. These experiments suggest that SP1 and SP2 consist of smaller metal oxide nano particles



capped by thioglycerol and drug respectively. Also it is observed that absorption of metal oxide is fairly sharp, which indicates the monodispersed nature of the nanoparticle distribution.

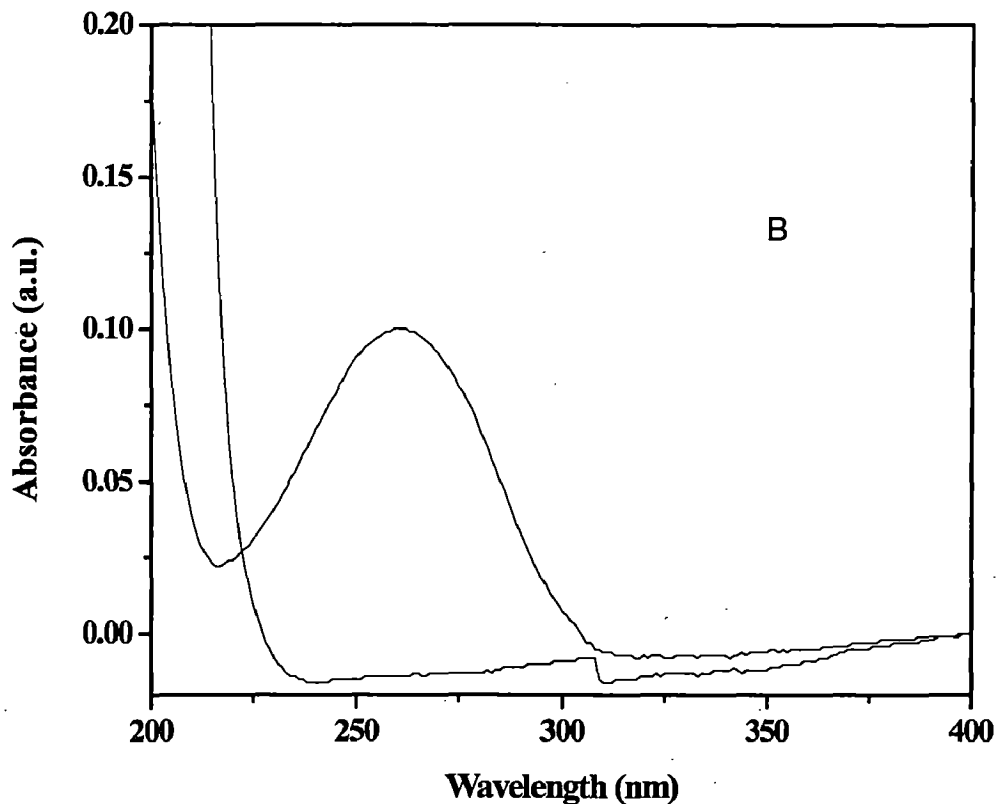


**Fig.5 UV-VIS Absorption Spectra of (A) SP1 Nanosystem (B) SP2 Nanosystem**

### **3.2a Emission Spectra of SP1 and SP2 Nanosystems**

The sample is excited at 290 nm and emission spectra recorded in the range of 300 nm – 600 nm. It shows a weak blue green emission peak (486 nm) and strong UV emission peaks (377 nm) but in case of SP2 nanoparticles a broad emission spectrum has observed in the UV-VIS region as shown in Fig.6. The emission at 377 nm corresponds to respective band gap of bulk material. This UV emission is assigned to the recombination of bound

excitons of metal oxide. The blue-green emission mechanism in these materials has been extensively investigated [58]. Single ionized oxygen vacancy has been considered to cause in green emission because of the recombination of a photo-generated hole with a single ionized electron in the valence band [20]. All the spectra in this study showed high UV emission and low blue-green emission. The high UV to visible emission ratio indicates a good crystal quality of the nanoparticles, *i.e.* a low density of surface defects.

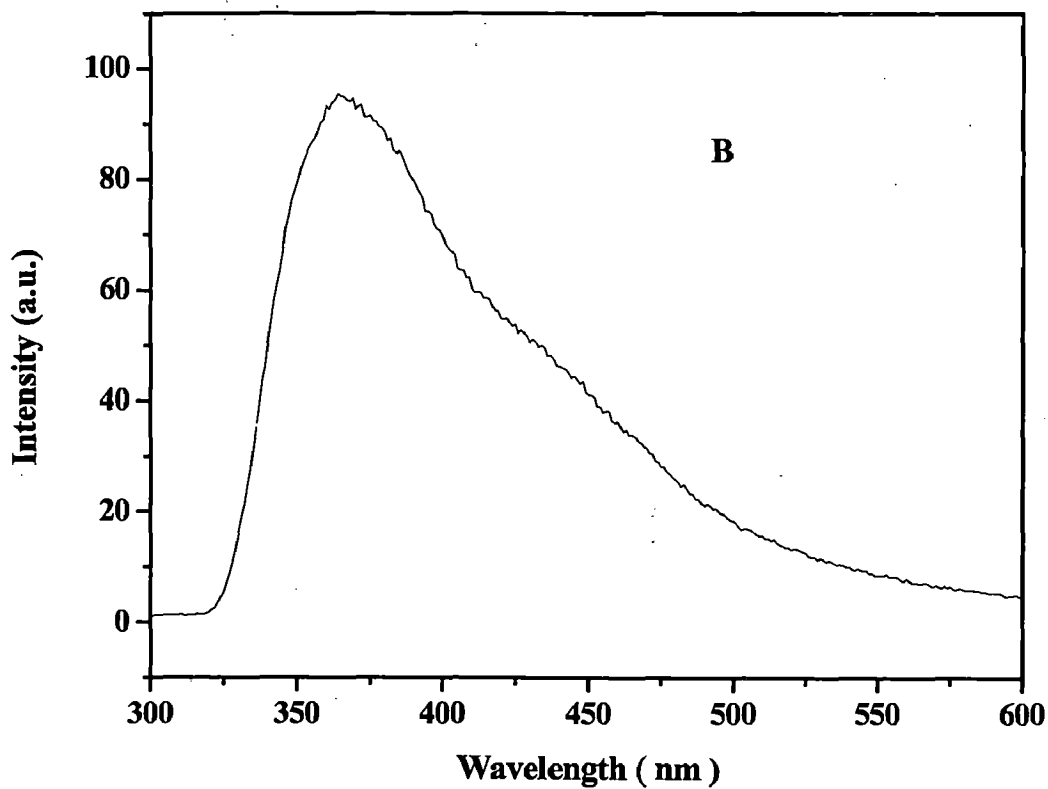


**Fig 6: Emission Spectra of (A) SP1 Nanosystem (B) SP2 Naosystem**

### **3.2 b Fluorescence Lifetime Decay curves**

Fluorescence lifetime decay was observed for the SP1, SP2 and the SP3 nanoparticles and it was found to be 7.12 ns, 7.49 ns and 6.19 ns respectively as shown in fig.6B

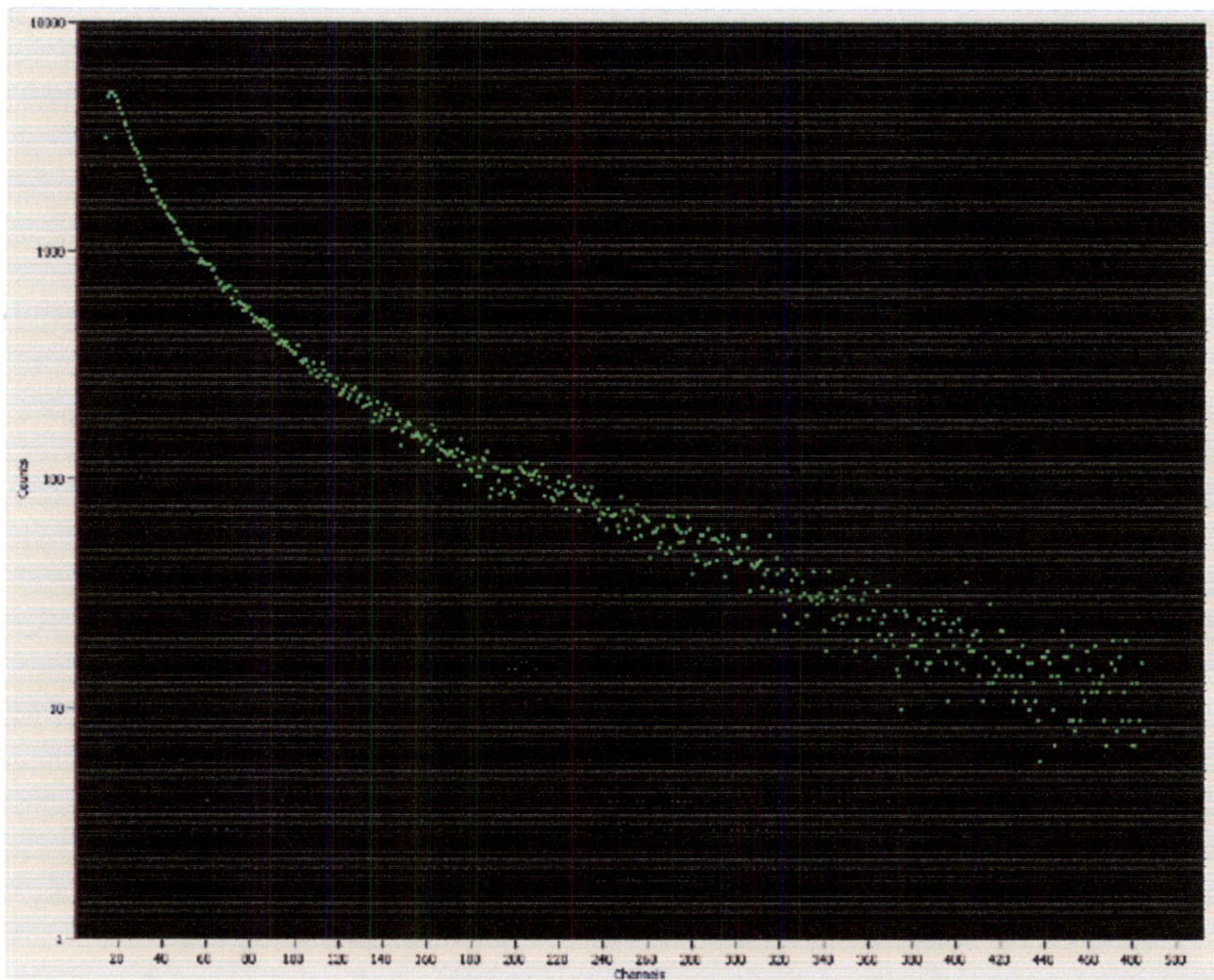


*Fig. 6A: Fluorescence Lifetime Decay of SPINanosystem.*

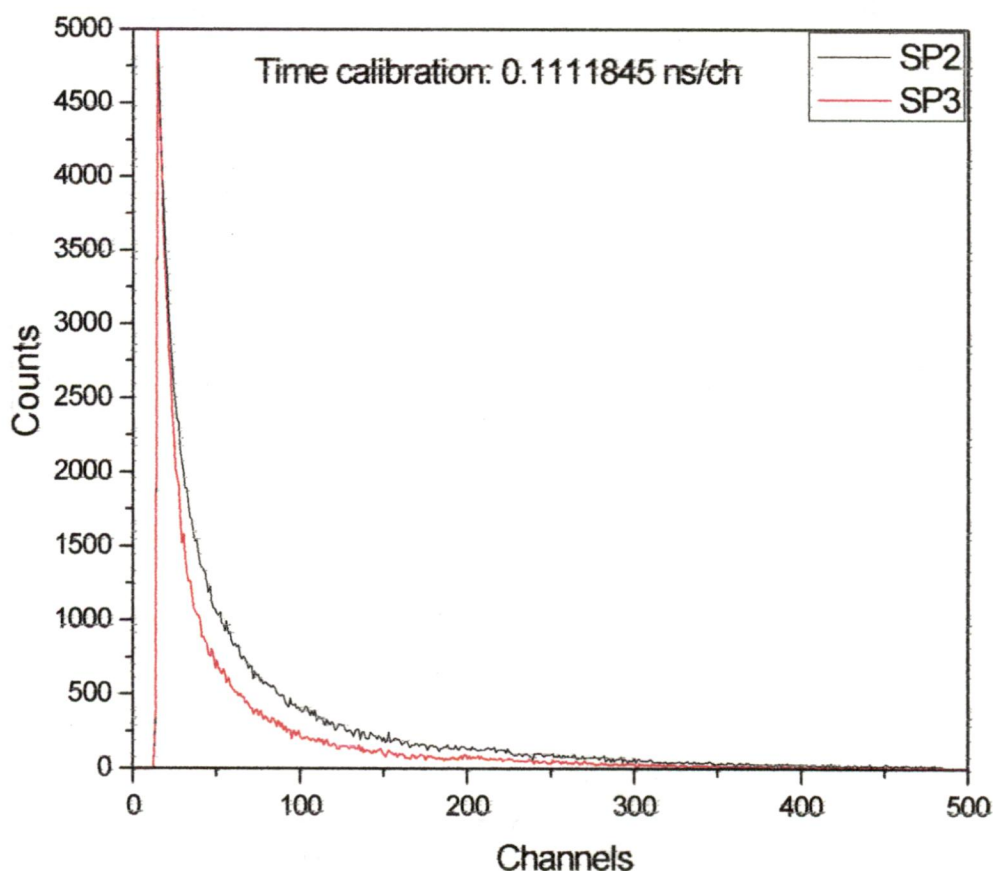
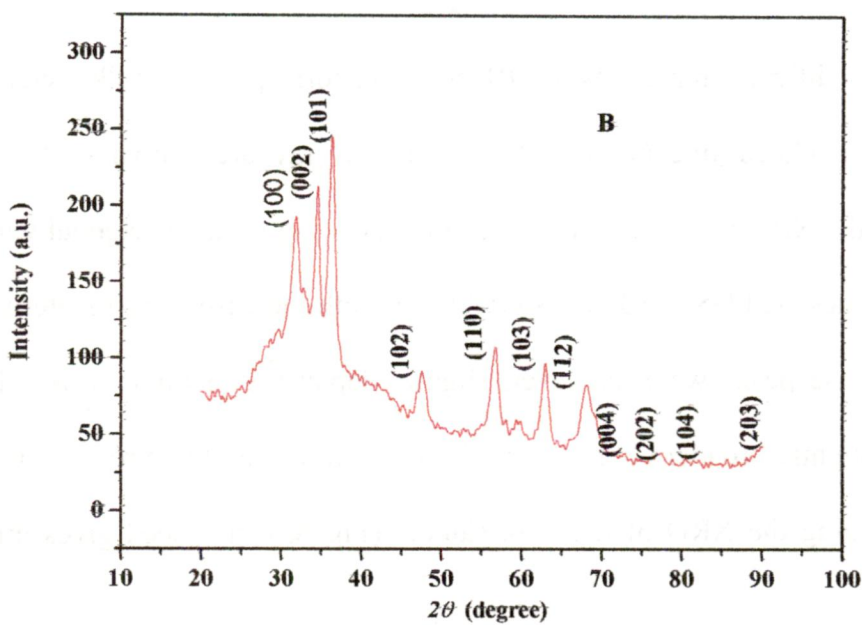
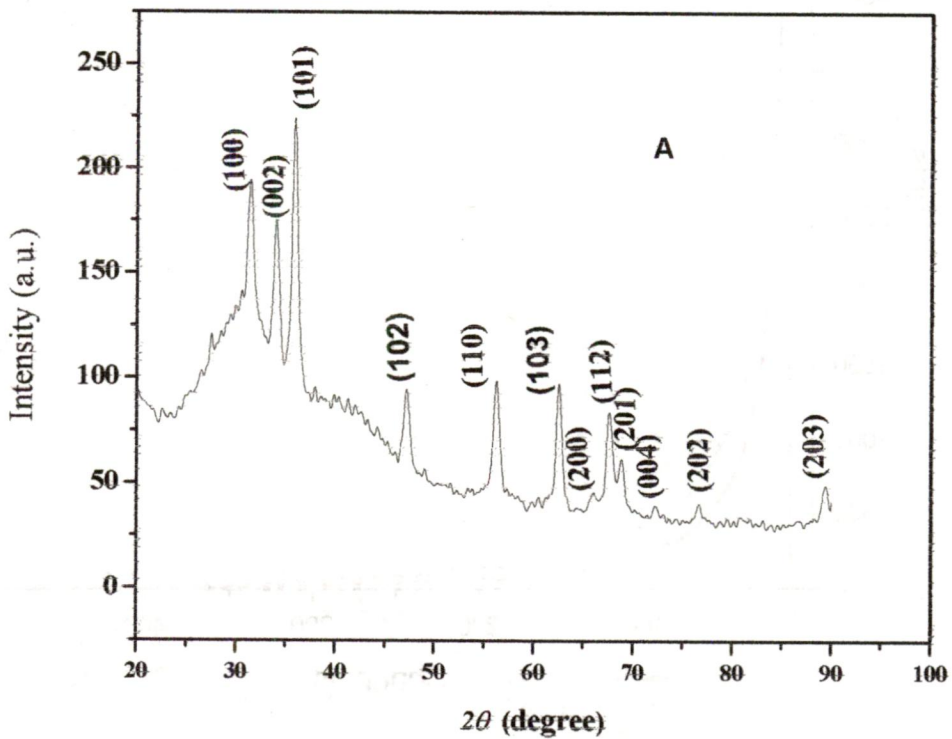


**Fig.6B: Fluorescence Lifetime Decay of SP1 SP2 and SP3 Nanosystems.**

### **3.3 X-Ray Diffraction**

The X- ray diffraction patterns of SP1, SP2 and corresponding bulk metal oxide, were recorded by using CuK $\alpha$  line (1.5418 Å) of the X- ray are shown in Fig.7. In these experiments, all the XRD peaks were indexed corresponding to the hexagonal wurtzite phase of used metal oxides (JCPDS Card No. 80-0075), in both the cases XRD pattern depict very similar peaks. These peaks were, however, slightly depict very similar peaks. These peaks were, however, slightly broader compared to those given in the literature data. It was further verified by recording the XRD of the bulk sample (Fig.7C). It indeed gives much sharper

reflection corresponding to different observed planes. The broadening of peaks in the present case suggests the as synthesized samples to contain relatively smaller sized particles.



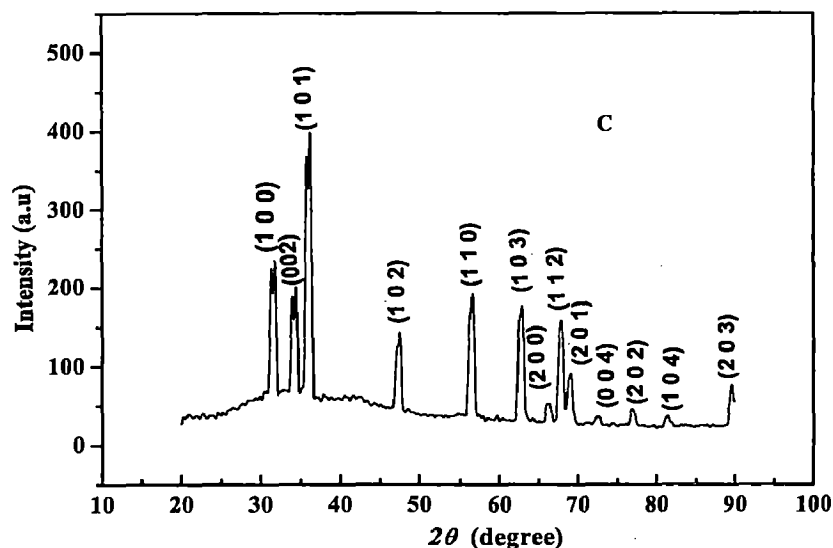


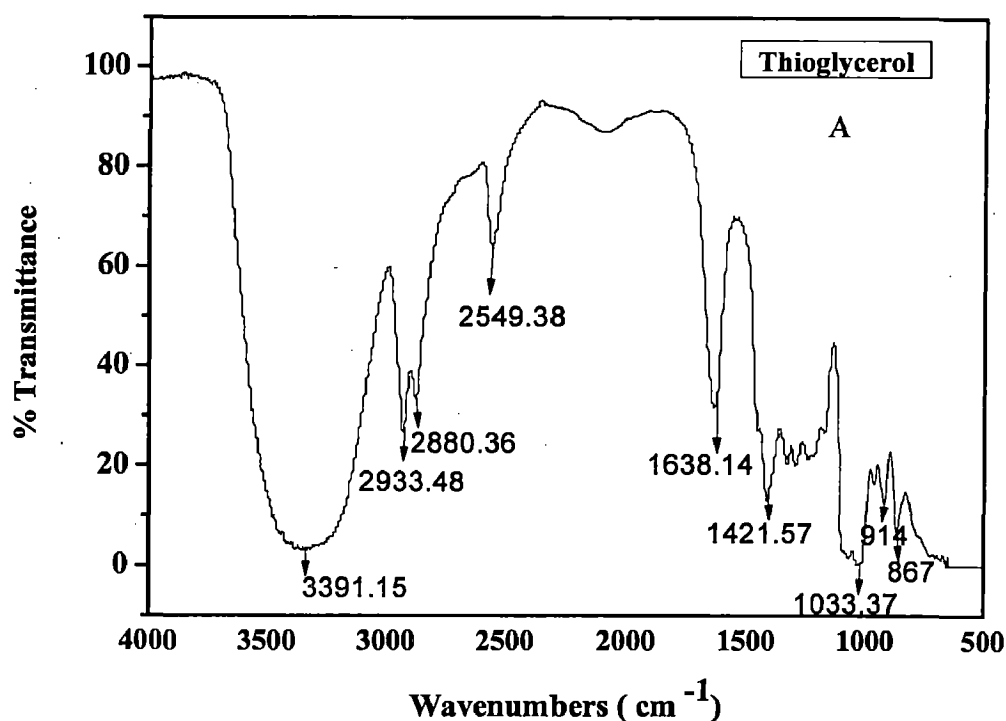
**Fig. 7: XRD pattern of (A) SP1 (B) SP2 and (C) Bulk material**

The particle size of SP1 and SP2 were also determined using the Scherrer formula [59]. The average particle size for SP1 and SP2 were found to be 12 nm and 10 nm respectively.

### **3.4 FTIR Spectroscopy of Samples**

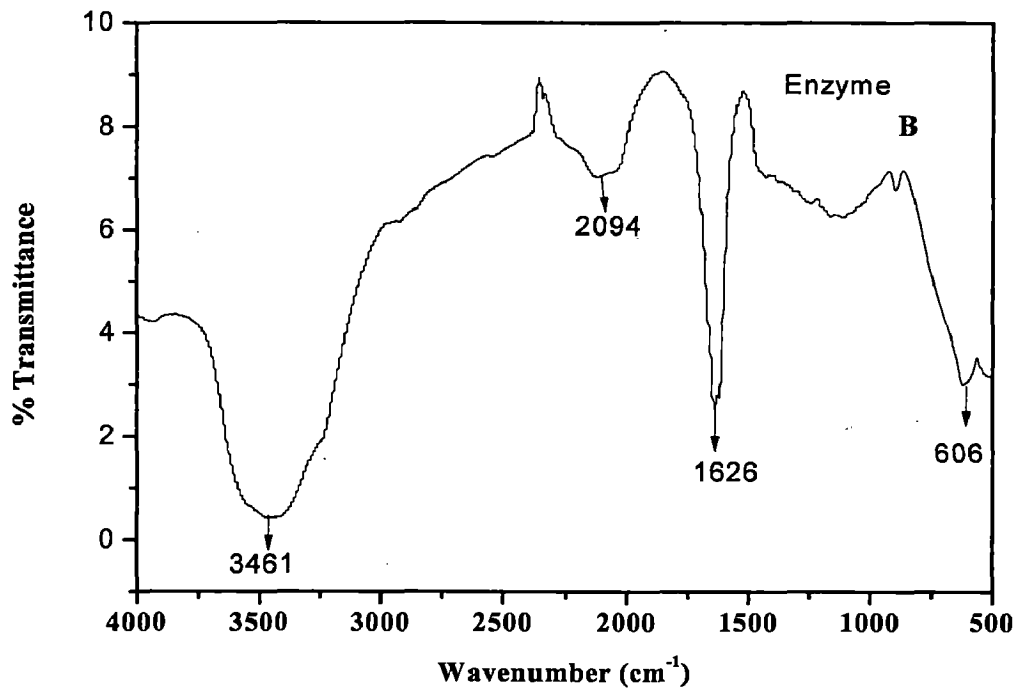
Figure 8 shows the FTIR spectrum for TG, E1, D1, SP1, SP2, SP3 and bulk metal oxide as shown in 8A, B, C, D, E, F, and G, respectively which contains nanoparticles coated by TG ( $\text{cm}^{-1}$ ), did not show all the vibrational bands due to TG as observed in 9A. Specifically, the peak due to  $-\text{SH}$  group ( $2549 \text{ cm}^{-1}$ ) observed disappeared completely and the broad band due to  $-\text{OH}$  group ( $3391 \text{ cm}^{-1}$ ) is shifted higher wavenumber, rest of all the peaks showed a marginal shifts in energy. Suggesting an interaction of TG with metal oxide. A comparison of the IR spectra of SP2 with that of the D1, reveal a change in the absorption corresponding to  $-\text{NH}$  group and  $-\text{OH}$  group in pure drug (D), a sharp bending vibration due to  $-\text{NH}$  is diminished and become fairly broad with a shifts to higher energy, the peak due to

-OH group remains very similar in the shape but exhibit, a shift in absorption to high energy. These changes reveal the interaction of metal oxide with the drug (D1) through -NH and OH groups. SP3 exhibits all vibrational features as observed in SP2 except it exhibits a sharp peak  $2064\text{ cm}^{-1}$  and a broad band between  $3200\text{-}3700\text{ cm}^{-1}$  indicating that it depicts an increased interaction with E1 as their bands at  $2094\text{ cm}^{-1}$  and  $3461\text{ cm}^{-1}$  are shift to lower energy ( $2064\text{ cm}^{-1}$ ). The band due to -OH has now become fairly broad. Thus, IR studies reveal that ZnO Nanoparticles interact with all the compounds TG, E1 and D1.

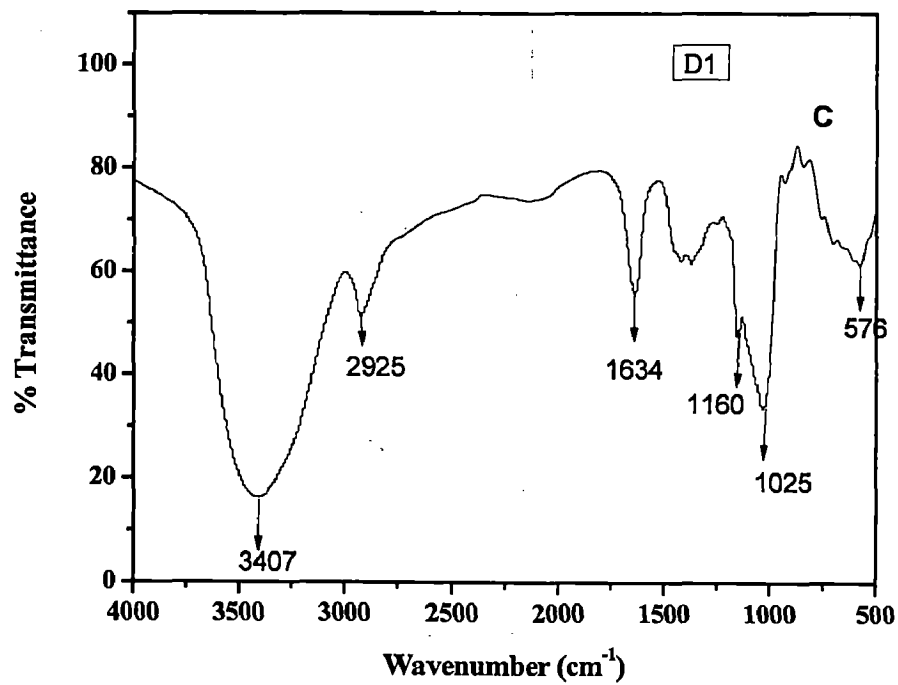


**Fig.8A: IR Spectrum of TG**



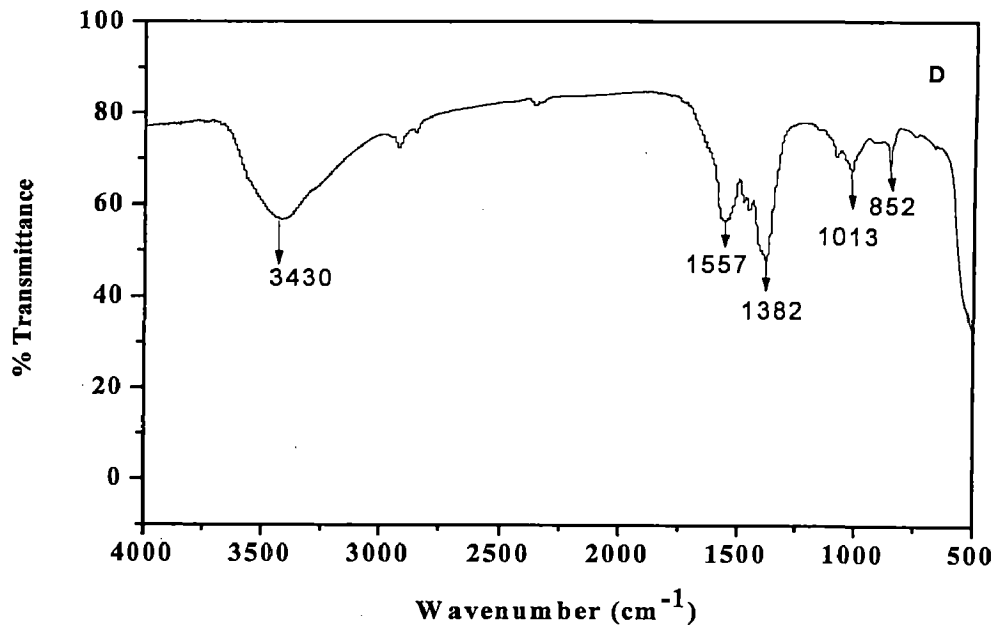


*Fig.8B IR Spectrum of E1*

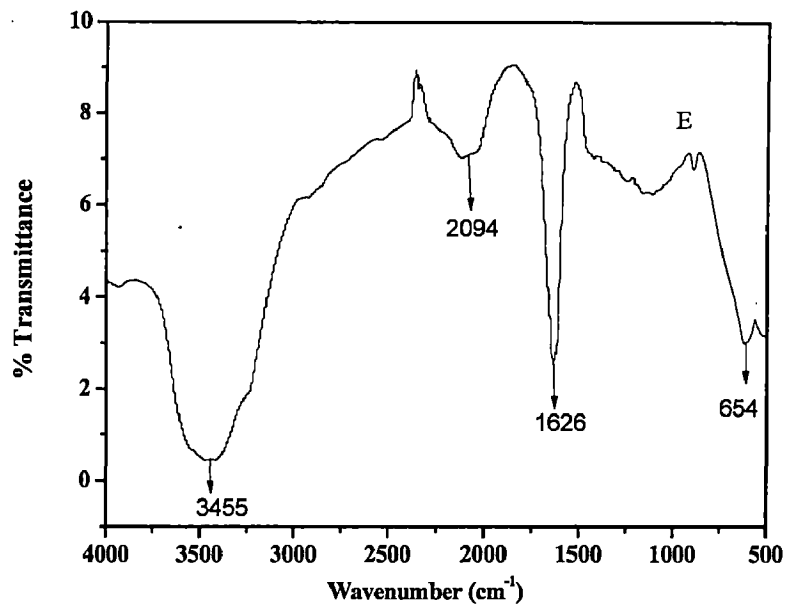


*Fig.8C IR Spectrum of D1*

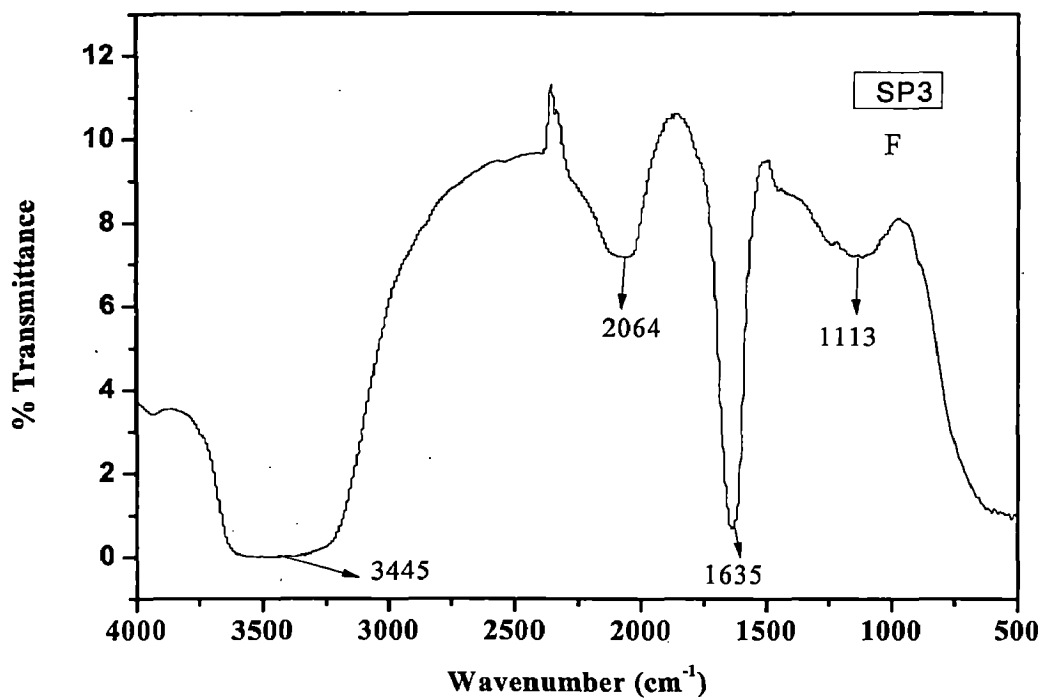




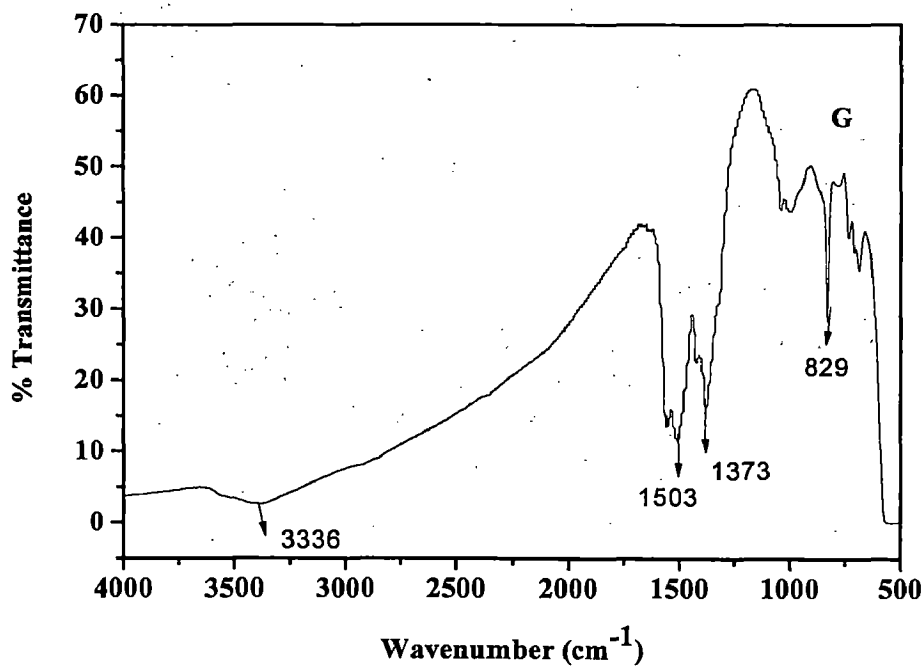
*Fig. 8D IR Spectrum SP1 Nanoparticles*



*Fig. 8E IR Spectrum of SP2 Nanosystem*



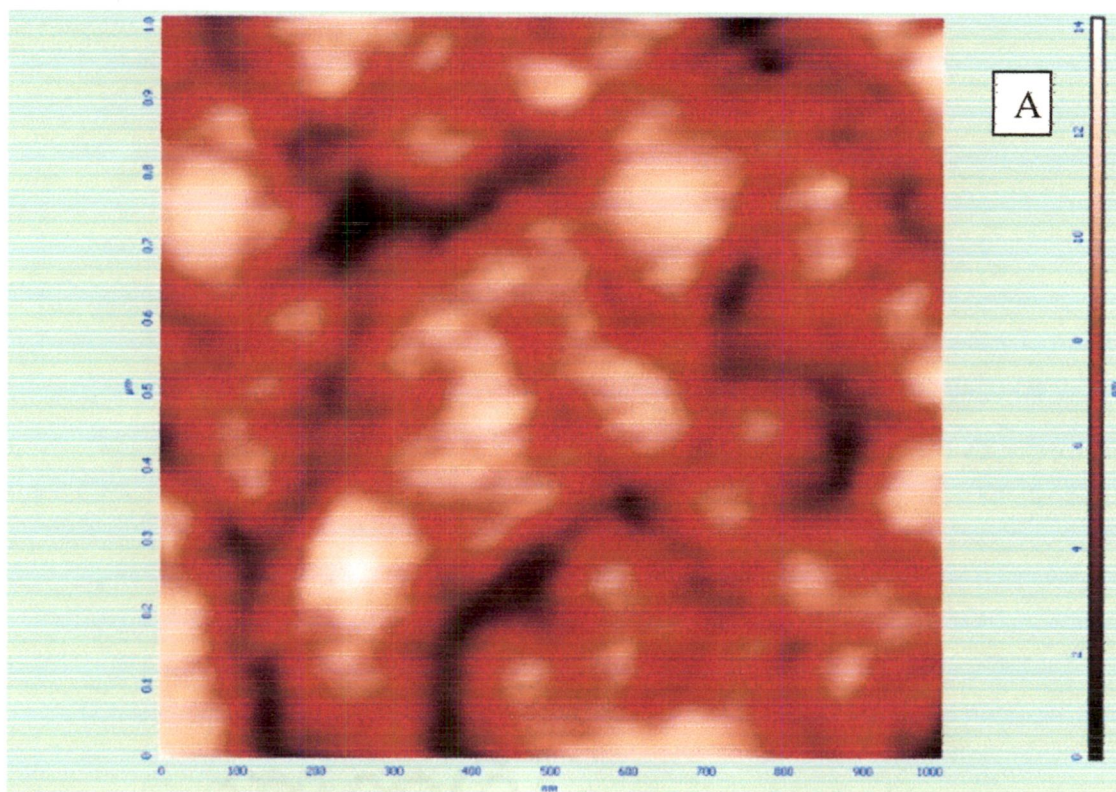
*Fig. 8F IR Spectrum of SP3 Nanosystem*



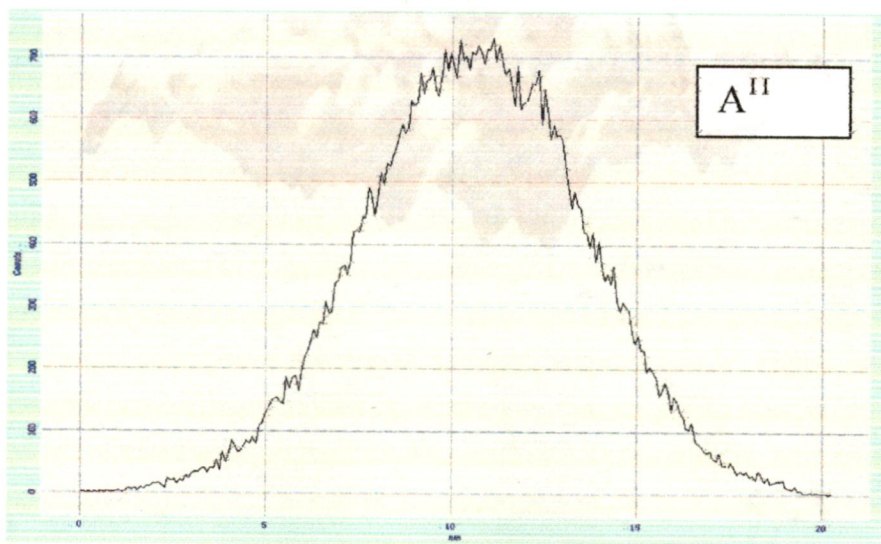
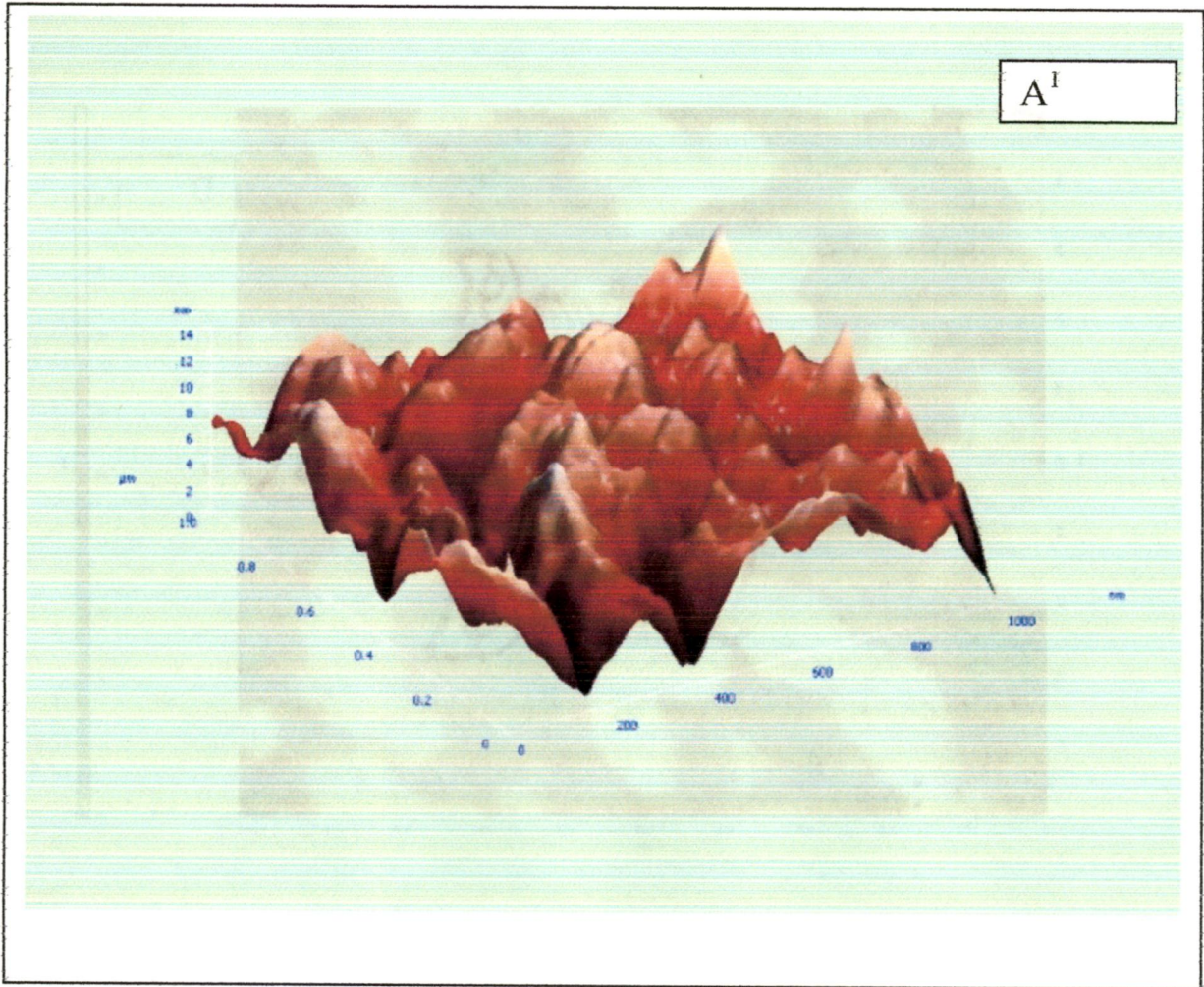
*Fig. 8G IR Spectrum of Bulk Metal Oxide*

### 3.5 Morphology of Nanosystems

Fig.9 shows the 2D and 3D AFM images of SPI, SP2, SP2 +Enzyme (SP3) and enzyme (E1). For all the samples of AFM images consist of spherical particles with a slight difference in their organization. SP3 (Fig.9A) depicts the presence of chains of clusters consisting of spherical particles, whereas the sample E1 exhibits the presence of largely isolated spherical particles. However, for all other samples, comparison of surface roughness of these samples shown in fig. 9A<sup>11</sup>, B<sup>11</sup>, C<sup>11</sup> and D<sup>11</sup>, follow the order: E1 < SP2 < SP1 < SP3. A close examination of these images reveal that the drug coated nanoparticles in the presence of enzyme has the highest surface roughness, which is understood by the increase binding of particles with the enzyme.

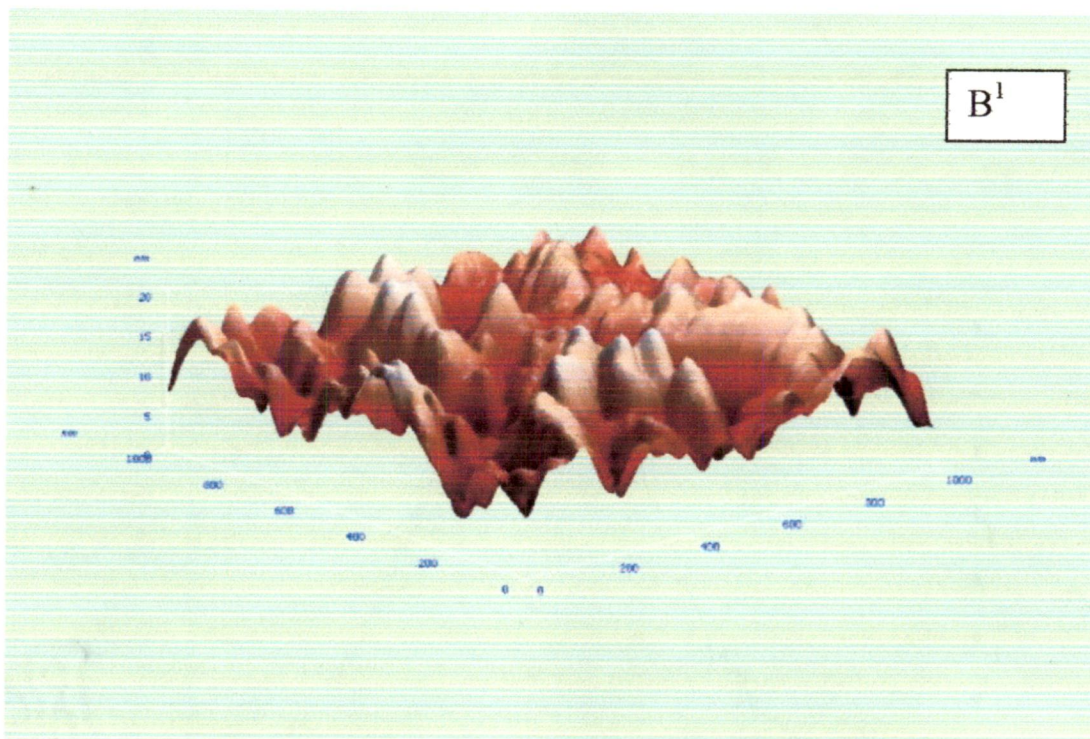
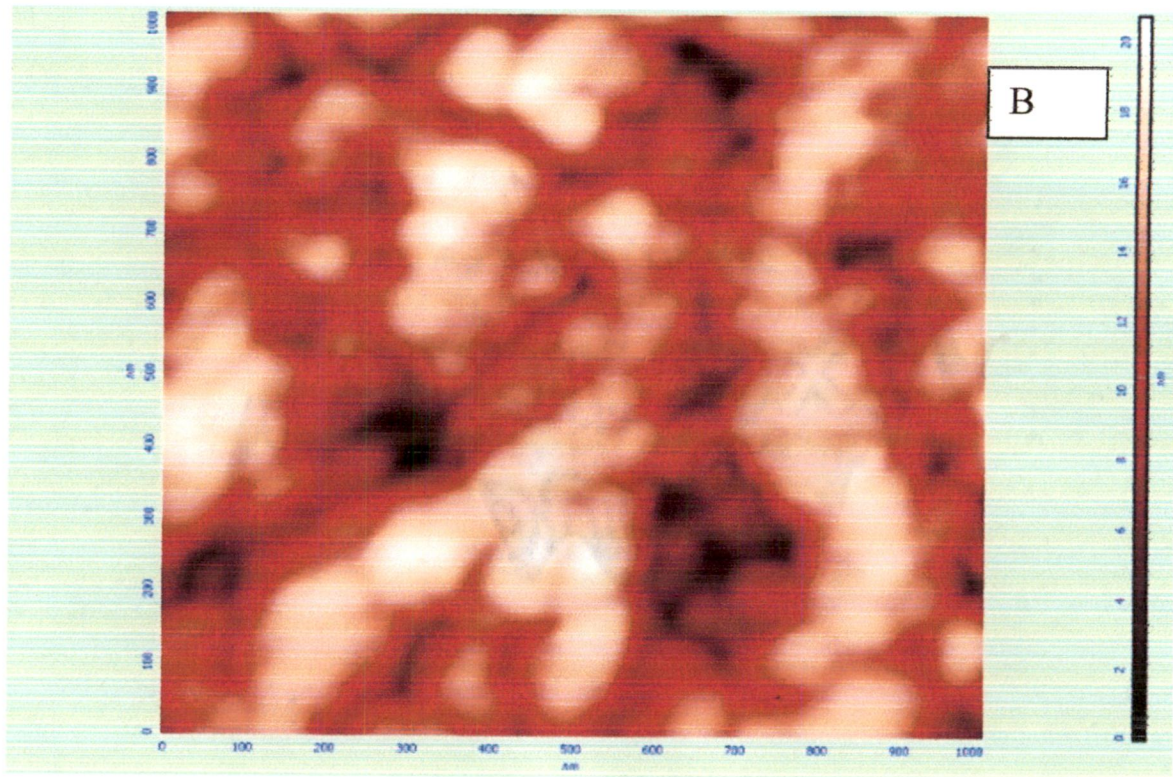




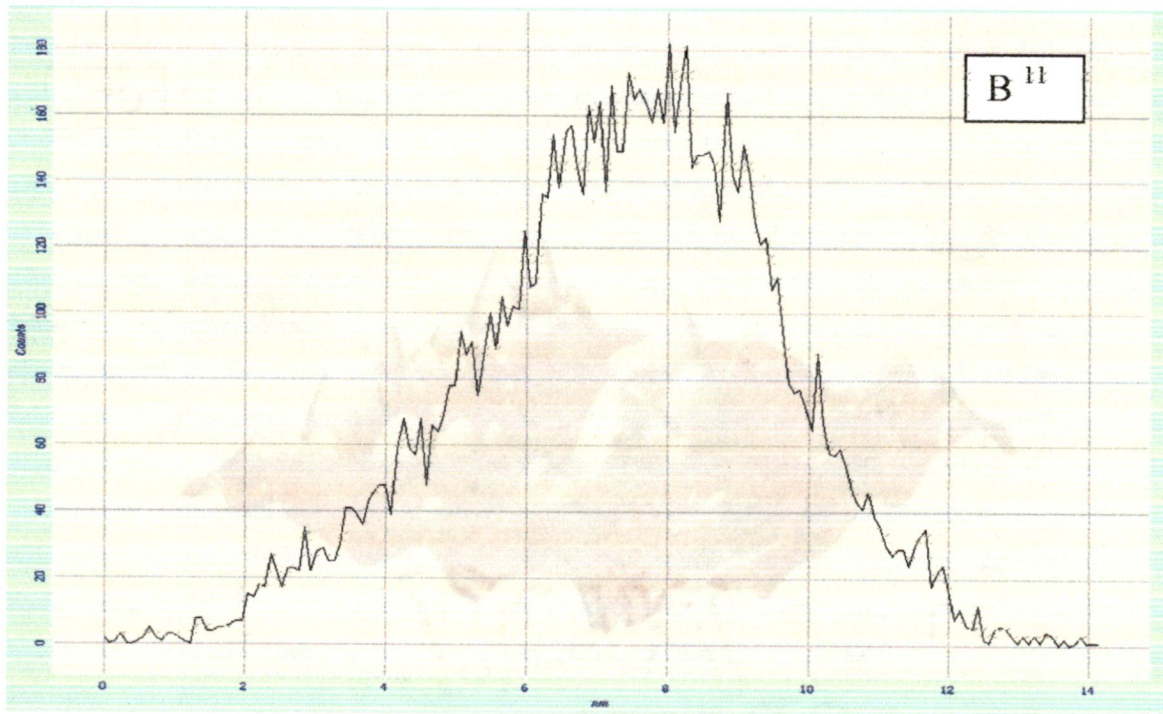


**Fig. 9A: SPI Nanoparticles**

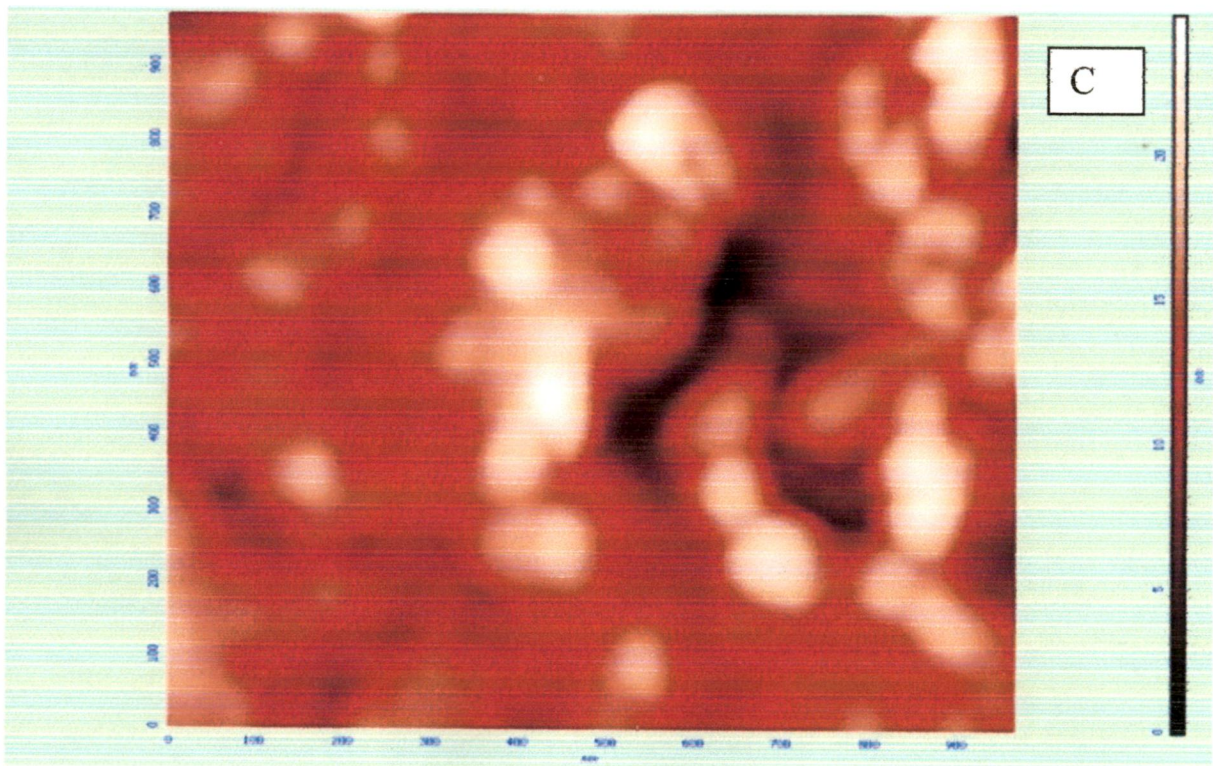




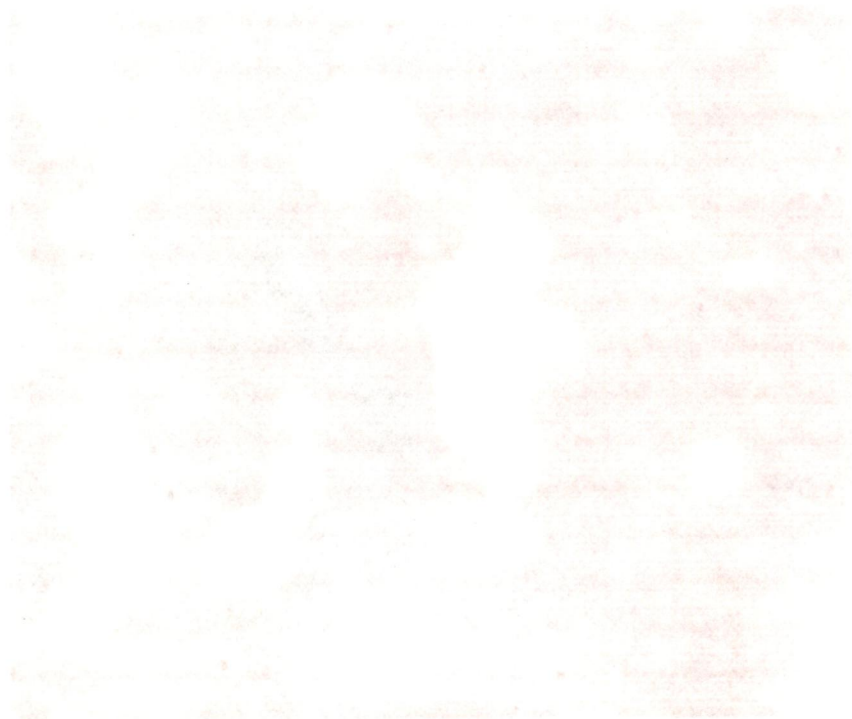
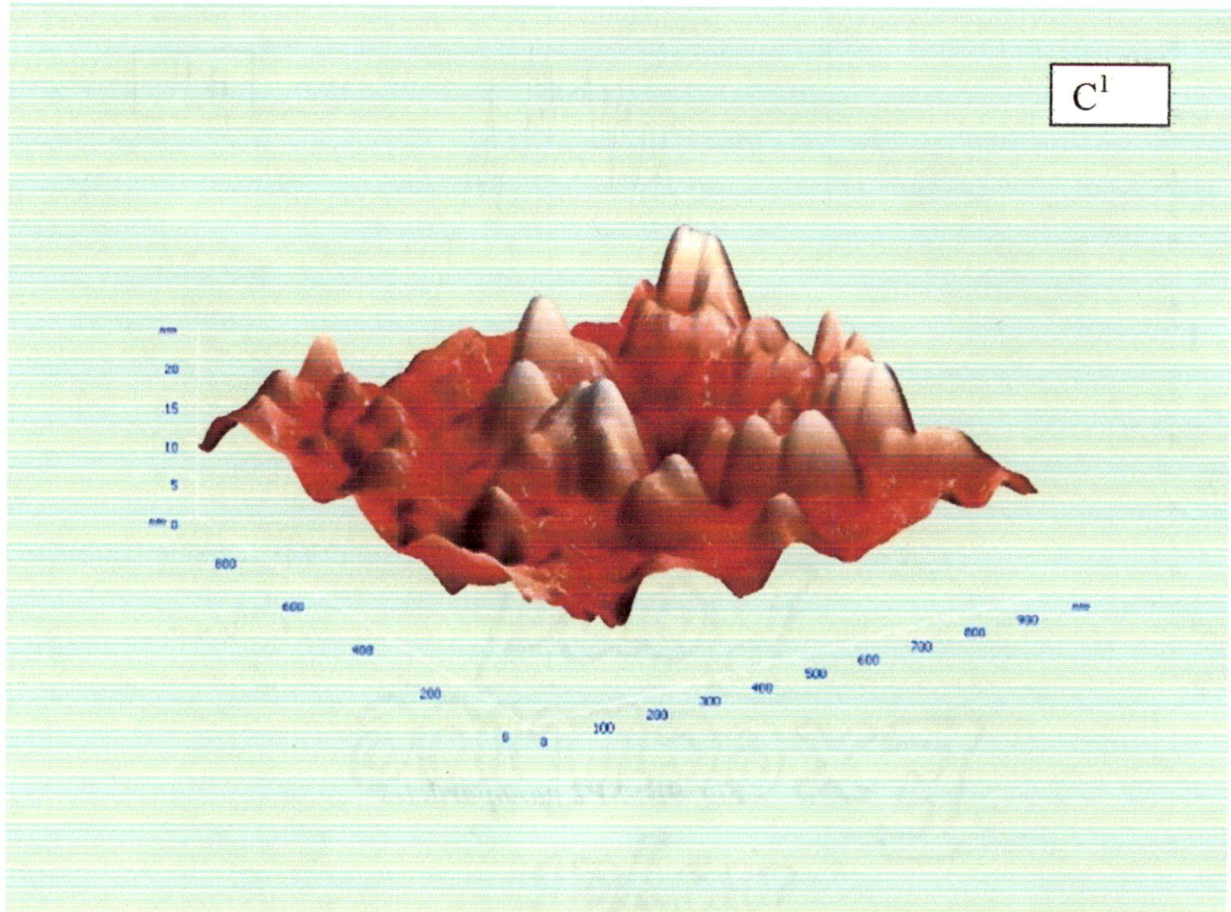




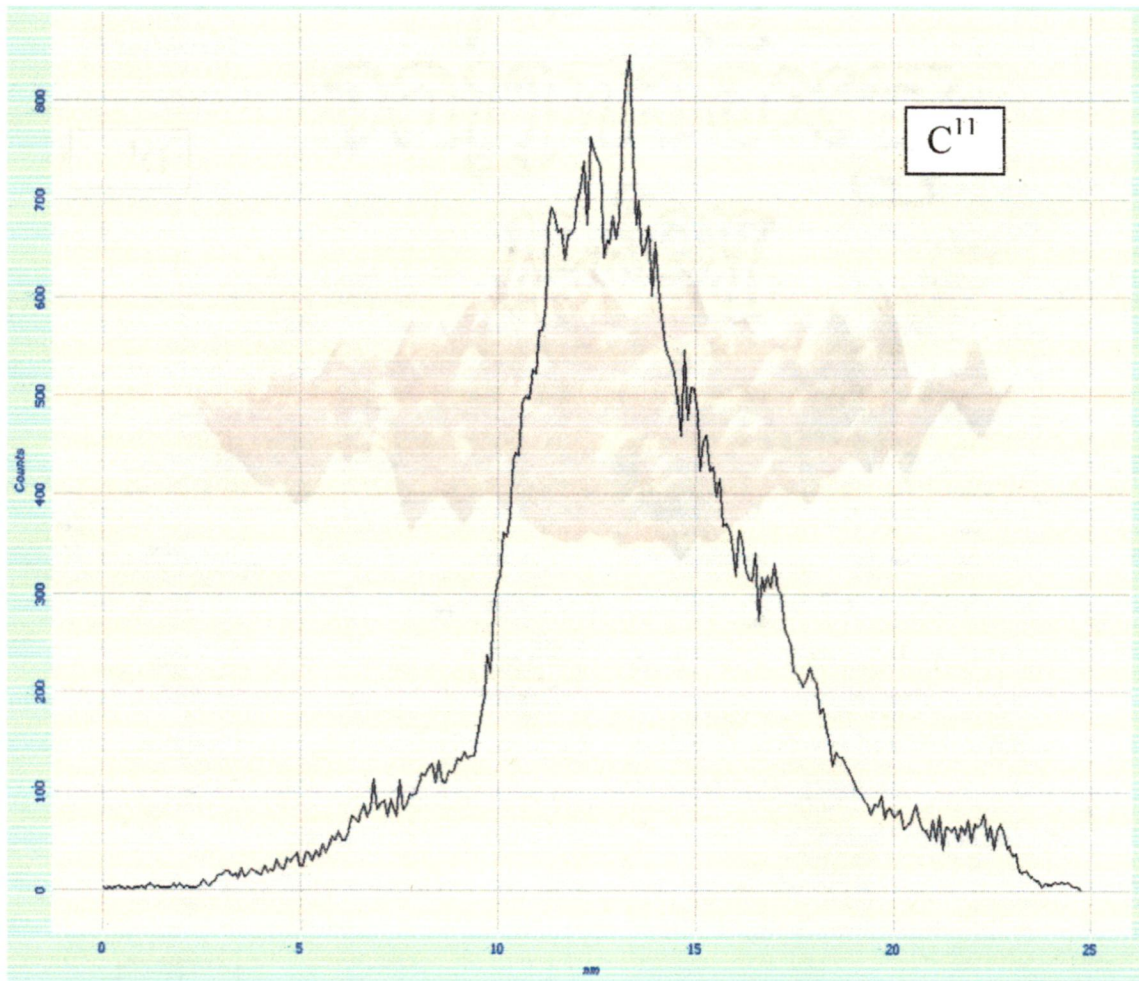
*Fig. 9B: SP2 nanoparticles*



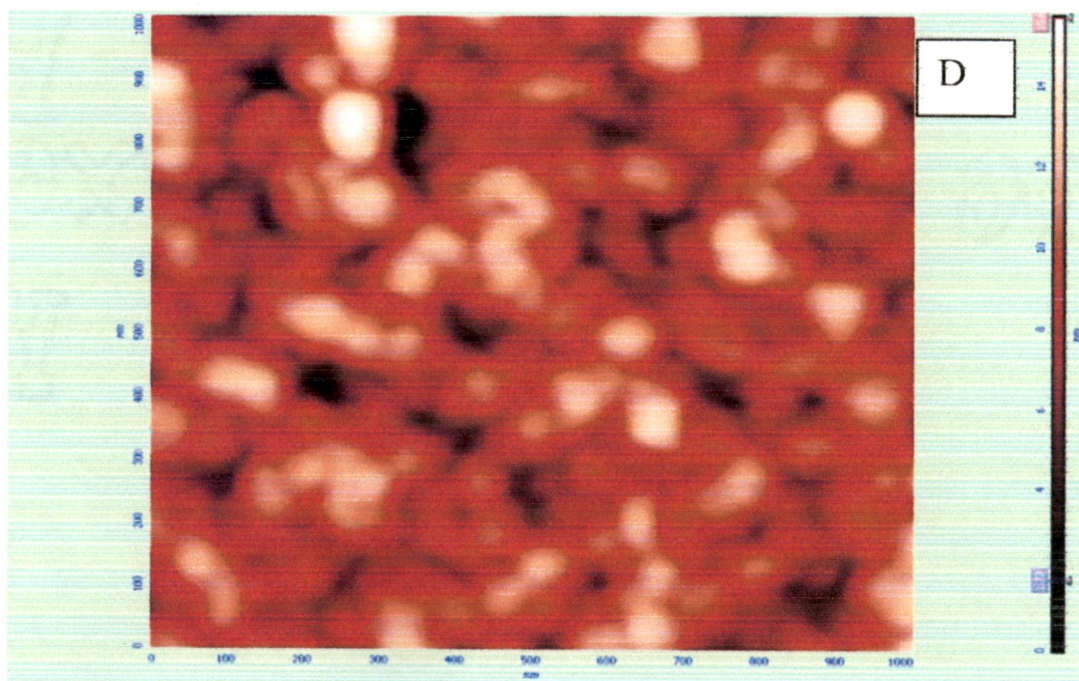
C<sup>1</sup>







*Fig.9C: SP<sub>3</sub> Nanosystem*





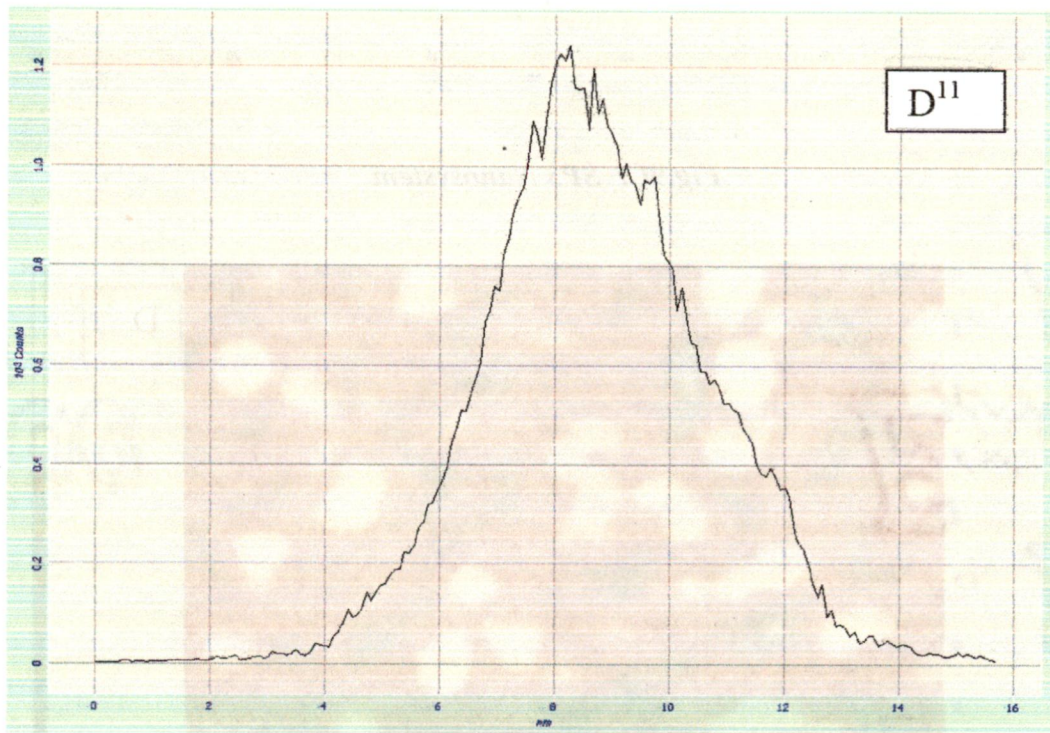
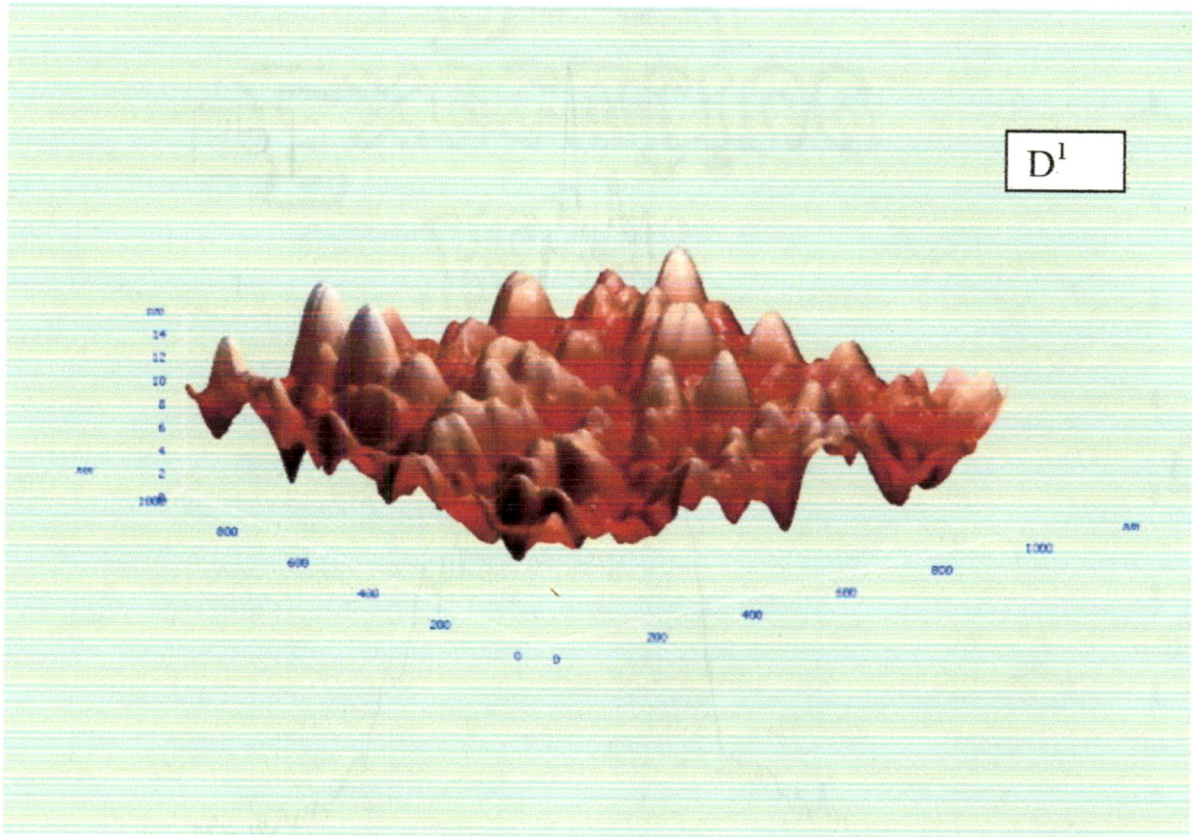
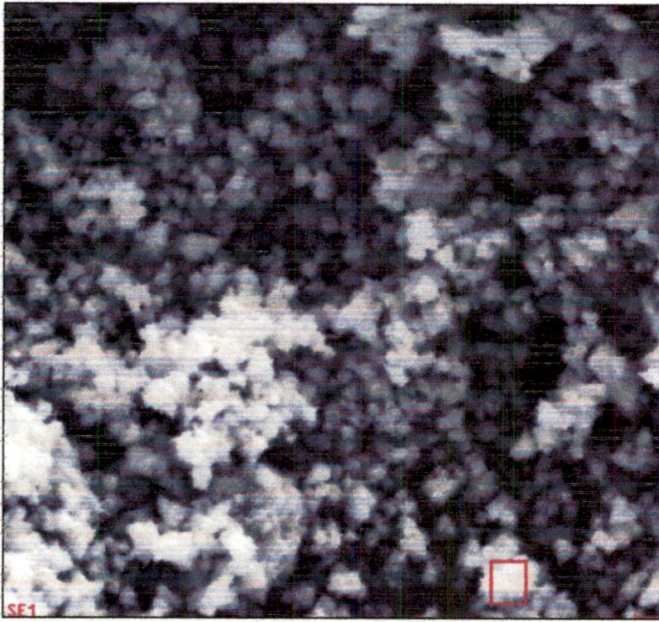


**Fig. 9D: Enzyme (E1)**





Element	Wt%	At%
CK	19.74	49.96
OK	08.71	16.56
SK	00.44	00.42
ZnK	71.11	33.07

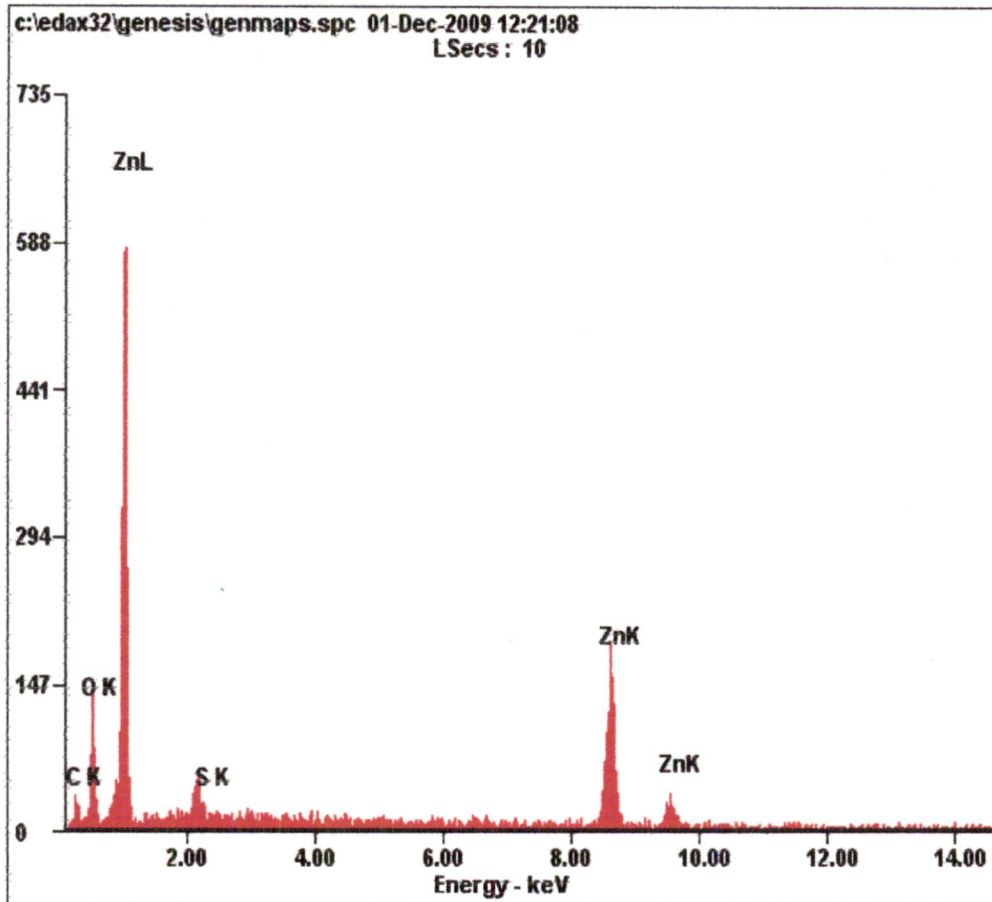
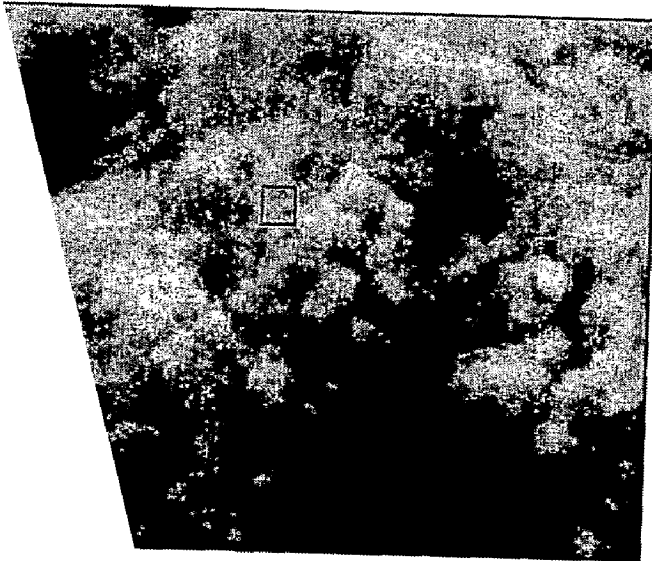
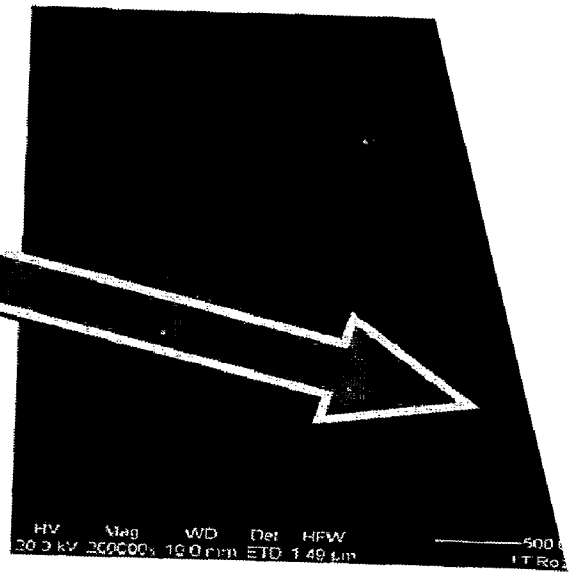
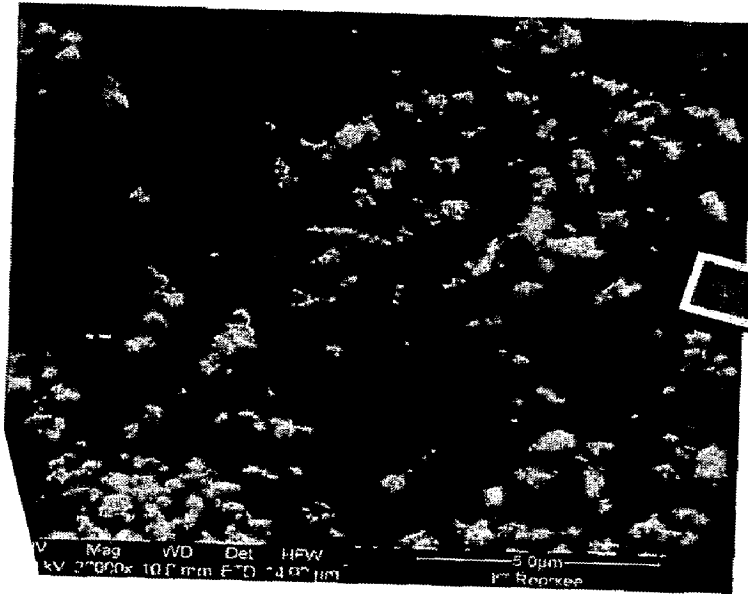


*Fig. 10B: EDAX spectra SPI Nanosystem*





<b>Element</b>	<b>Wt%</b>	<b>At%</b>
<b>CK</b>	31.08	55.37
<b>NK</b>	01.10	01.69
<b>OK</b>	20.54	27.47
<b>ZnK</b>	47.27	15.47

**Fig. 10.1A: FESEM of SP2 Nanosystem**

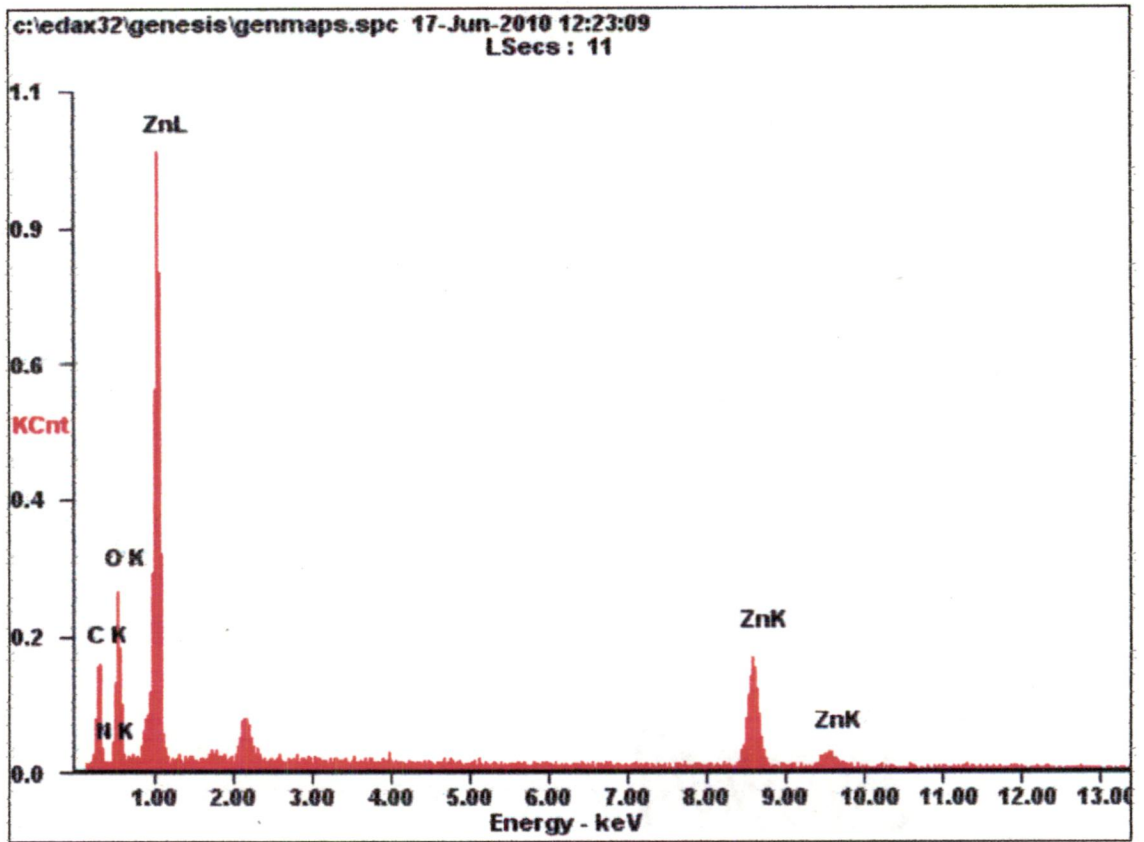
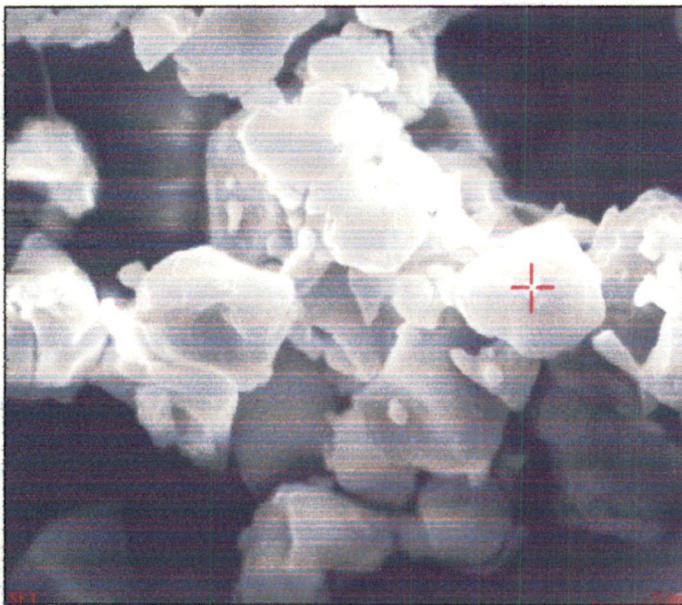


*Fig. 10.1B: FESEM of SP2 Nanoparticles*



Element	Wt%	At%
CK	68.21	73.40
NK	08.05	07.43
OK	23.73	19.17

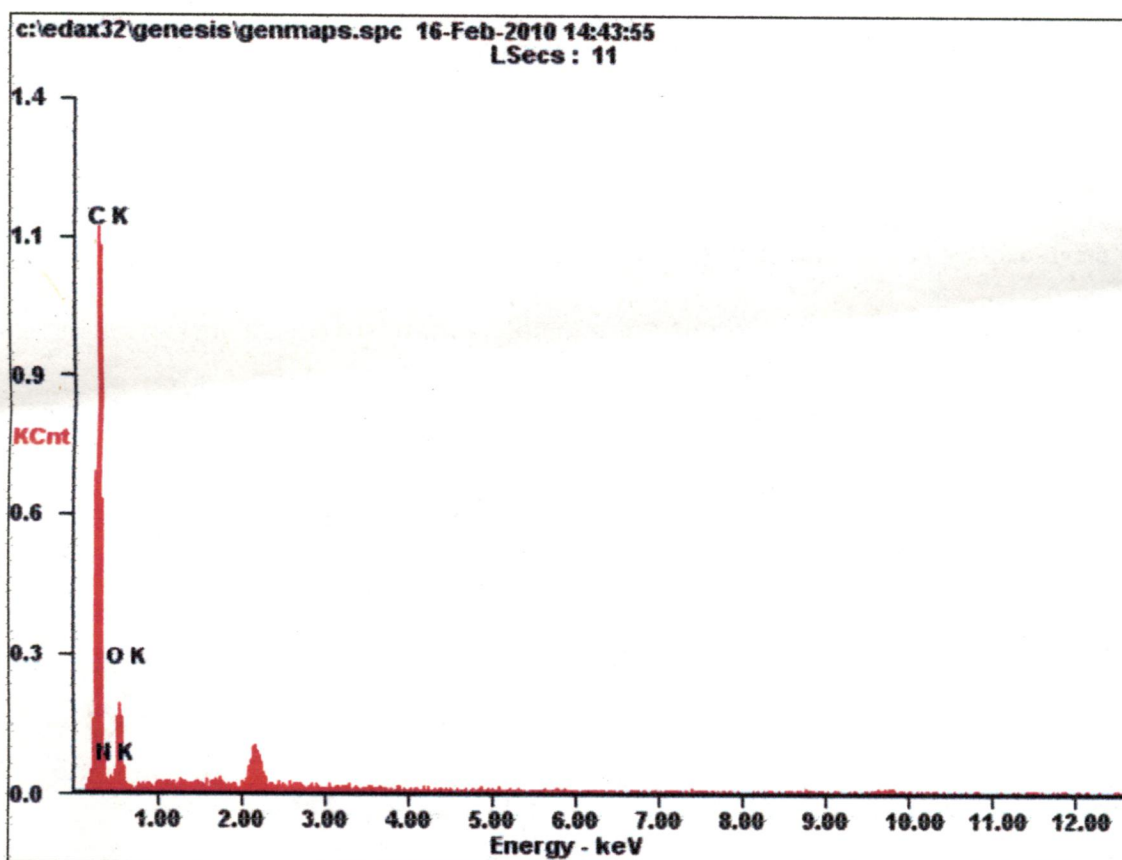


*Fig. 10C: FESEM and EDAX of Drug*

### ***3.7 Inhibitory Activity of SP1 and SP2 Nanosystems***

In order to examine inhibitory activity of different designed nanosystems a series of experiments involving the optimization of amount of starch, amount of nanoparticles, effect of temperature, and effect of pH were performed. For a specific enzyme activity about 0.16 mg / ml (Fig. 11A) was found to produce the maximum amount of sugar, in all other subsequent experiments this amount of starch and activity were maintained constant. For SP1 nanosystems the amount of capped nanoparticles was worked by monitoring percentage inhibition as a function of its amount. From this experiment, the maximum percentage of inhibition corresponded to 30  $\mu\text{g}$  / mL of SP1 (Fig.11B). For this system percentage of

inhibition was monitored by varying the temperature and pH from (20-50 °C) and pH(s) (3-9) respectively. From these experiments, the optimized temperature and pH were found to be 36 °C and 7, respectively (Figs.11D&E). The inhibition effect was checked with nanoparticles produced by two different batch systems and checked by taking readings for three times of each sample and the inhibition is reproducible with relative standard deviation  $\pm 2\%$ . Similar experiments were designed with SP2 nanosystem and sample of D. Plots for inhibitory action for the drugs and SP2 nanosystems are presented in fig.11C & fig.11F, respectively. Upon examination of these plots, the higher inhibitory activity was observed with drug. Thus, comparison, of all the plots for inhibitory activity of SP1 and SP2 nanosystems reveal that maximum inhibitory was obtained with SP2 with relative standard deviation of  $\pm 1.5\%$ . Interestingly, nanoparticles alone without drug also demonstrate an inhibition activity. To the best of our knowledge the first report on inhibition action of nanoparticles with glycosidases.

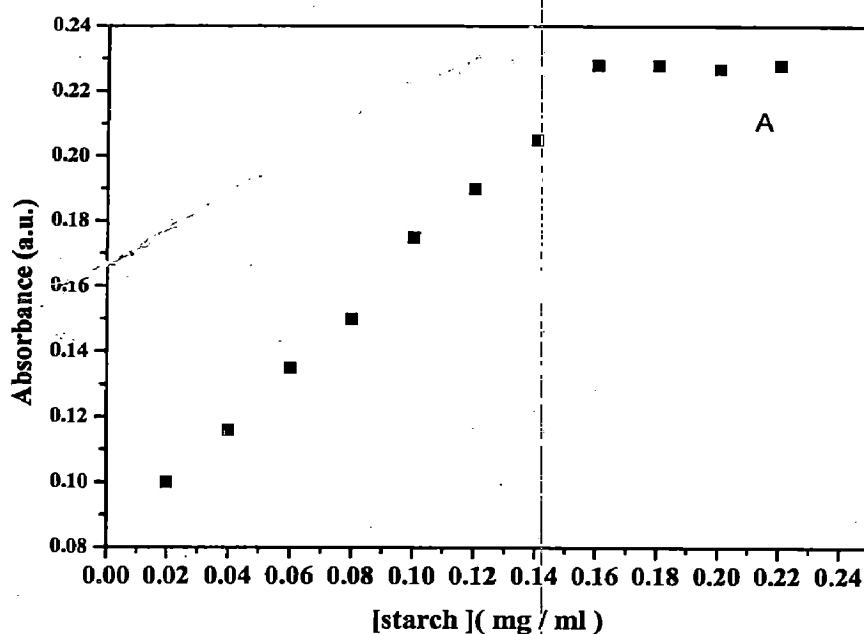


**Fig. 11A: Effect of [Starch] on Enzyme Activity**

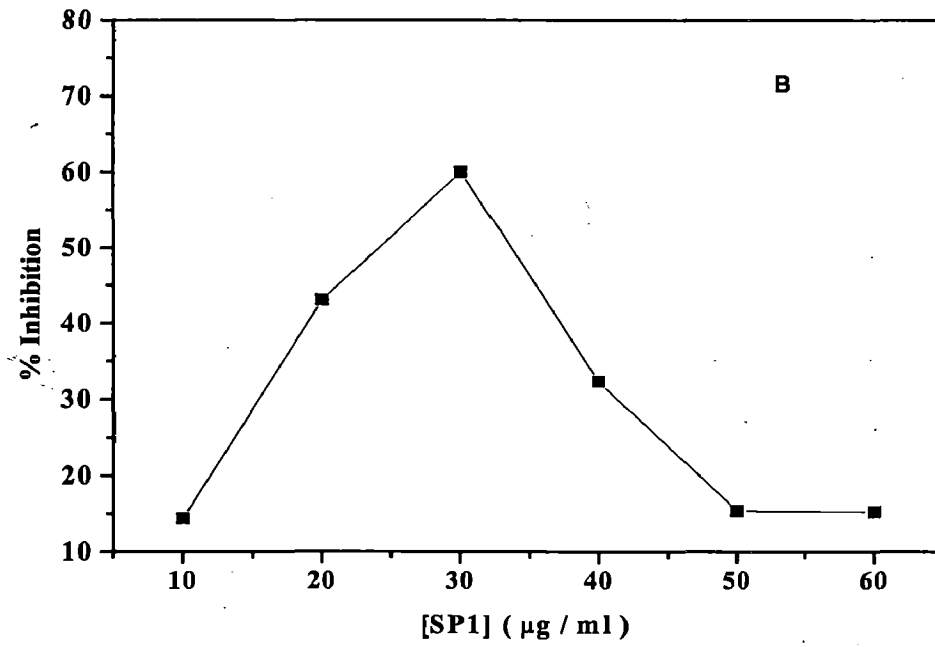


**Fig.11B: Effect of [SP1] on Enzyme Activity**

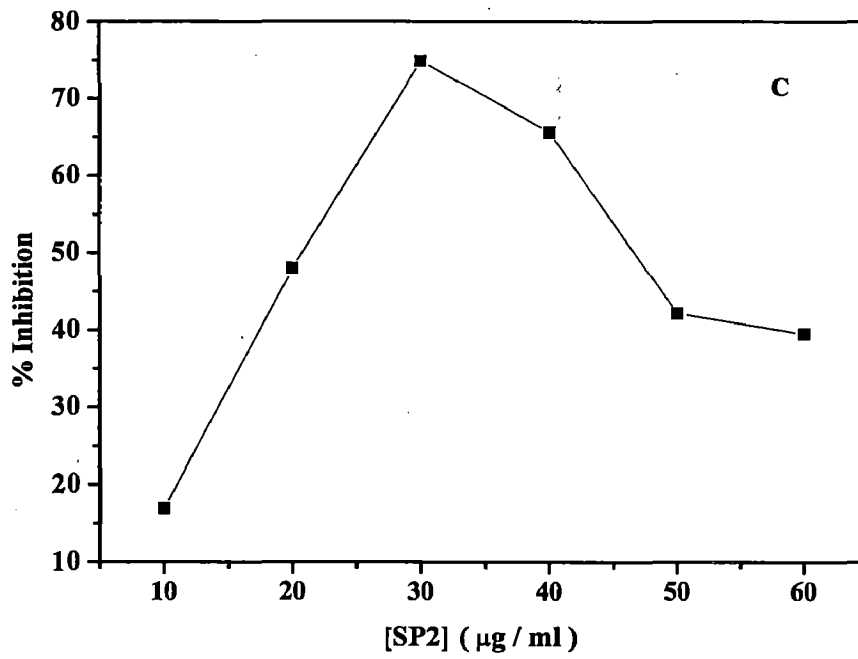


**Fig .11C: Effect of [SP2] on enzyme activity**



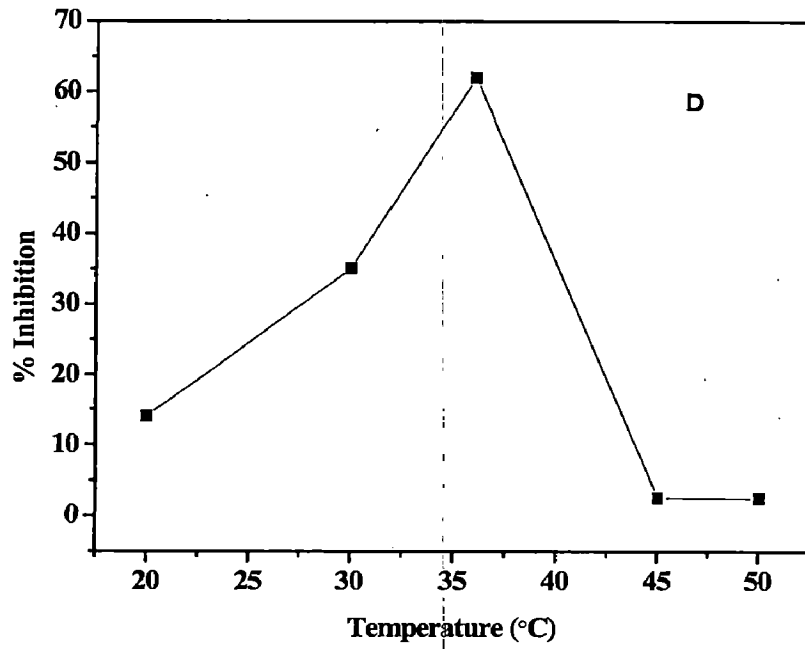


**Fig. 11D: Effect of temperature on inhibitory action of nanoparticles on Enzyme Activity**

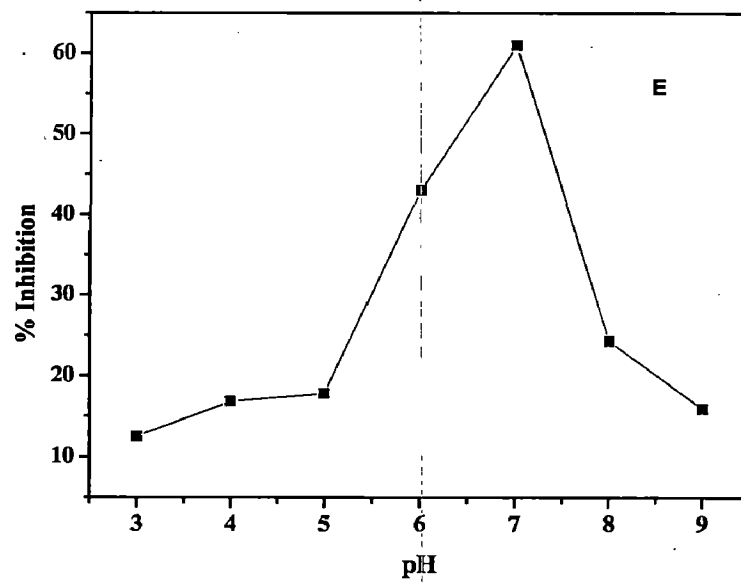


**Fig 11E: Effect of pH on Inhibitory Action of Nanoparticles on Enzyme activity**

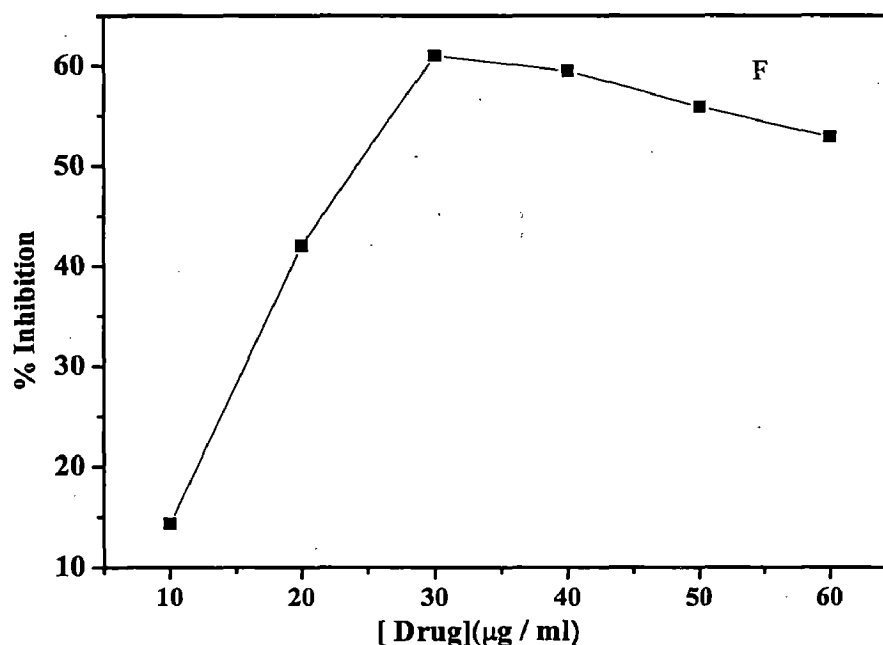


**Fig 11F: Effect of [Drug] on Enzyme Activity**

### **3.8 Discussion**

We have successfully synthesized thioglycerol and drug modified metal oxide nanoparticles. The formation of nanoparticles has been confirmed from the characteristic features studied by optical and emission spectroscopy, XRD, FESEM and AFM studies. The electronic spectra (Figs.5A & 5B) exhibit an onset of absorption at 323 nm (3.83 eV) and 320 nm (3.875 eV), which lie at much higher energy compared to the band edge of respective bulk material ( $E_g = 3.3$  eV). Moreover, the excitonic absorption(s) recorded in the present case are also at higher energy with respect to that of bulk. These data clearly suggest the formation of nanosized metal oxide nanoparticles in the present case. The appearance of the intense band gap emission (3.2 eV) compared to the emission arising from defect states (2.5 eV) further indicate the synthesized nanosystems to contain small size particles compared to that of bulk.

A reduction in the size of these particles in the presence of the TG matrix and the drug is assigned to the interaction between metal oxide and these entities which is clearly evidenced by performing the FTIR spectroscopy in their presence and absence. These studies have demonstrated the interaction of nanoparticles through –OH and –SH; –NH and –OH in the cases of chemically and drug modified particles, respectively. Change in size and morphology of metal oxide nanoparticles further supports the surface interaction between them, which lead to the size quantization through surface modification. The observed similarity in inhibition activity of enzyme by SP1 with the standard drug suggests these particles to behave in a similar fashion to that of the drug. An enhancement in inhibition activity in the conversion of carbohydrate to glucose is understood by the increased interaction between the enzyme and SP2, which is supported by the above presented analysis by AFM, FESEM, emission and FTIR studies.

### ***3.9 Conclusion***

We have synthesized chemically and drug modified nanoparticles successfully. These particles were characterized by AFM, FESEM, and XRD, which demonstrated them to be spherical. Both of these nanosystems have been used to examine the inhibitory action of glycoside hydrolases for the production of glucose from starch. For the glycoside hydrolases, nanoparticles alone exhibited the novel inhibition activity, which is observed to be very similar that of standard drug being used presently for the purpose. A combination of both nanoparticles and drug is found to enhance the inhibitory action further by about 30 %. The developed nanosystems represent a new class of materials in the field of biomedicine, for which the preliminary investigation suggests them to be the prospective drug, which could response / supplement the existing standard drug. However, these materials needed to be

explored more critically in vivo system as regard for their toxicity, side effects and combined effect of various other biochemicals present in the metabolic environment prior to their usage.

### 3.10 References

1. Ratner M., and Ratner D. "*Nanotechnology: A Gentle Introduction to the Next Big Idea*" 2003 PrenticeHall PTR 1st edition.
2. [www.nanoroadmap.it/events/first\\_conference/presentations/bax.pdf](http://www.nanoroadmap.it/events/first_conference/presentations/bax.pdf)
3. [www.sps.aero/Key.../TSA-001\\_Dendrimers\\_White%20Paper.pdf](http://www.sps.aero/Key.../TSA-001_Dendrimers_White%20Paper.pdf)
4. Klabunde, K.J. (Ed.), *Nanoscale Materials in Chemistry*, John Wiley & Sons Inc., New York, 2001.
5. Scherer, G. W., 'Theory of Drying,' *J. Am. Ceram. Soc.*, 73 [11] 3-14 (1990).
6. Anil Kumar, " Physico chemical and photochemical properties of nanoscale semiconductors" lead article, *National academy science letter*, 28, 1-11 (2005).
7. Pradeep, T., *NANO: The essentials, understanding nano science and technology*, Tata Mcgraw-Hill, 2008.
8. Jaiswal, J. K.; and Simon, S. M., *Trends in Cell Biology* 14, 9 (2004).
9. Azzazy, H. M. E et al. *Clinical Biochemistry* 40, 917–927 (2007);
10. Boieriu, P., Sporken, R., Xin, Y., Browing, N.D. and Sivananthan, S., " Wurtzite CdS on CdTe grown by molecular beam epitaxy," *J. Electron. Matter.* 29,718 (2000).
11. Sulieman, K.M., Huang, X., Liu, J. and Tang, M., " One-step growth of ZnO/ZnS core shell nanowires by thermal evaporation," *Smart Mater.Struct.*, 16, 89 (2007)
12. Zhai, T., Fang X., Bando, Y., Liao, Q., Xu, X., Zeng, H., Ma, Y., Yao, J. and Golberg, D., " Morphology –dependent stimulated emission and field emission of ordered cds nanostructure arrays," *ACS Nano*,3,949 (2009)
13. Chen, C.-H., " Self- organized InGaN nanodots grown by metal-organic chemical vapour deposition system," *Opt.Rev.* 16, 367 (2009).

14. Taneja, P., Vasa P. and Ayyub, P., "Chemical passivation of sputter-deposited nanocrystalline CdS thin films," *Mater. Lett.*, 54, 343 (2002).
15. Fascko, S., Dekorsy, T., Koerdt, C., Trappe, C., Kurz H., Vogt, A. and Hartnagel, H.L., "Formation of ordered Nanoscale semiconductor dots by ion sputtering," *Science*, 285, 1551 (1991).
16. Morales, A.M and Lieber, C. M., "A laser ablation method for the synthesis of crystalline semiconductors nanowires," *Science*, 279, 208 (1998).
17. Schmid, G., "Nanoparticles," Wiley – VCH Verlag GmbH and Co, KGaA, Weinheim Press, Germany (2004).
18. Kar, S., Santra, S. and Heinrich, H., "Fabrication of high aspect ratio core shell CdS-Mn/ZnS nanowires by a two step solvothermal process," *J.Phys.Chem. C*, 112, 4036(2008).
19. Chen, Y., Zhang, X., Jia, C., Su, Y. and Li, Q., "Synthesis and characterization of ZnS, CdS, and composition – tunable  $Zn_xCd_{1-x}S$  alloyed nanocrystals via a mix-solvothermal route," *J.Phys, Chem.*, 113, 2263(2009).
20. Li, H. And C., "Sonochemical synthesis of cyclodextrin-coated quantum dots for optical detection of pollutant phenols in water," *Chem. Matter.*, 20, 6053(2008).
21. Roy, M.D., A Herzing, A.A., Lacerdaa, S.H.D.P. and Becker, M.L., "Emission-tunable microwave synthesis of highly luminescent water soluble CdSe/ZnS quantum dots," *Chem. Commun.*, 2106 (2008).
22. Panda, A.B., Glaspell, G. And El-Shall, M.S., "Microwave synthesis of highly aligned ultra narrow semiconductors rods and wires, *J.Am. Chem.Soc*, 128, 2790 (2006).

23. Maitheu, H., Richard, T., Aligre, J., Lefebvre, P. And Arnaud, G., " Quantum confinement effects of CdS nanocrystals in a sodium borosilicate glass prepared by the sol-gel process," J. Appl. Phys.77, 287 (1995).
24. Marandi, M., Taghavinia, N., Irajizad, A. and Mahdavi, S.M., " Fine tuning of the size of CdS Nanoparticles synthesized by a photochemical method," nanotechnology, 17, 1230 (2006).
25. Zhao, W.-B., Zhu, J. J., and Chen, H.-Y., " Photochemical preparation of rectangular PbSe and CdSe Nanoparticles," J. Cryst. Growth, 252, 587(2003).
26. Chang, S.-Q., Kang, B., Dai, Y.-D. and Chen, D., " A novel route to synthesize CdS quantum dots on the surface of silk fibres via  $\gamma$ - radiation ," Mater.Lett.,62, 3447 (2008).
27. Sun, J. and Buhro, W.E., " The use of single –source precursors for the solution – liquid-solid growth of metal sulfide semiconductors nanowires, " Angew.Chem.Int.Ed., 47,3215 (2008).
28. Rajendran,V., Lehing,M. and Niemeyer, C.M., " Photocatalytic activity of colloidal CdS Nanoparticles with different capping ligands," J.Matter.Chem., 19, 16348 (2009).
29. Ma, N., Yang, J., Stewart, K.M. and Shana O.Kelley, S.O., " DNA- Passivated CdS nanocrystals: luminescence , bioimaging , and toxicity profiles ," Langmuir , 23, 1278 (2007).
30. Zhou, H., Fan, T., Zhang, Qixin Guo,Q. and Ogawa, H., " Novel bacteria –templated sonochemical route for the in situ one-step synthesis of ZnS hollow nanostructures," Chem.Mater., 19, 2144 (2007).

31. Lu, C., Cheng, Y., Liu, Y., Liu, F. And Yang, B., " A facile route to ZnS- polymer nanocomposite optical materials with high nanophase content via  $\gamma$ - irradiation initiated bulk polymerization ,” *Adv. Mater.* ,18,1188 (2006)
32. Zhao, Y., Zhang Y., Zhu, H., Hadjipanayis, G.C. and Xiao, J.Q., " Low-temperature synthesis of hexagonal (wurtzite) ZnS nanocrystals,” *J. Am. Chem. Soc.*, 126, 6874 (2004).
33. Lee, J. and Yoon, M., " Synthesis of visible light-sensitive ZnO nanostructures: sub wavelength waveguides,” *J. Phys. Chem. C*, 113, 11952 (2009).
34. Chen, X. and Mao, S.S., " Titanium dioxide materials: synthesis, properties, modifications and applications,” *Chem. Rev.*, 107, 2891 (2007).
35. Park, J., Lee, E., Hwang, N.-M., Kang, M., Kim, S.C., Hwang, Y., Park, J.-G., Noh, H.-J., Kim, J.-Y., Park, J.H and Hyeon, T., " One- nanometer-scale size-controlled synthesis of monodisperse magnetic iron oxide Nanoparticles,” *Angew. Chem. Int. Ed.* 44, 2872 (2005).
36. Barringer, E. A.; and Bowen, H. K. *J. Am. Ceram. Soc.* 65, 199-206 (1982).
37. Shi, L.; Li, C.; Chen, A.; Zhu, Y.; Fang, D. *Mater. Chem. Phys.* 66, 51-57 (2000).
38. Yin, S.; Sato, T. *Ind. Eng. Chem. Res.* 39, 4526-4530 (2000).
39. Liao, L. C.; Chiang, P. *Appl. Surf. Sci.* 253, 3982- 3986 (2007).
40. Ogihara, T.; Yanagawa, T.; Ogata, N.; and Yoshida. *J. Ceram. Soc.*,101, 315-320 (1993).
41. Kim, K. E.; Jang, S. R.; Park, J.; Vitta, R.; Kim, K. J. *Sol. Energy Mat. Sol. C*, 91, 366-370 (2007).
42. Barringer, E. A.; and Bowen, H. K. *Langmuir* 124, 414-420 (1985).



43. Dastjerdi, R., and Montaze, M., "A review on the application of inorganic nano-structured materials in the modification of textiles: Focus on anti-microbial properties" *Colloids and Surfaces B: Biointerfaces*.79, 5-18 (2010).
44. Özgür, Ü.; Alivov, Ya. I.; Liu, C.; Teke, A.; Reshchikov, M. A.; Doğan, S.; Avrutin, V.; Cho, S.-J. *et al.* "A comprehensive review of ZnO materials and devices". *Journal of Applied Physics* 98, 7 -18 (2005).
45. Baruah, S. and Dutta, J. "Hydrothermal growth of ZnO nanostructures" *Sci. Technol. Adv. Mater.* 10, (2009).
46. J.Q.Hu, J.Q., Wong N.B., Lee, S.T., " Synthesis of uniform hexagonal prismatic ZnO whiskers," *Chem.Mater.*, 14, 1216 (2002).
47. Xiang, H.-M., G. Shchukin, D.G., Mohwald, H., Xu, Y. and Xia. Y.-Y., " Sonochemical synthesis of highly luminescent Zinc Oxide Nanoparticles doped with Magnesium (II)," *Angew.Chem.Int.Ed.* 48, 2727 (2009).
48. Zhang, L., Sunil., Yin, J., Su, H., Liao, C. and Yan, C., " Control of ZnO morphology via simple solution route," *Chem.Matter.*, 14, 4172 (2002).
49. Tian, Z.R., Voigt, J.A., Liu, J., Mckenzie, B., and Mcdermott, M.J., " Biomimetic arrays of oriented helical ZnO nanorods and columns," *J.Chem.Soc.* 124, 12954 (2002).
50. Carnes, C.L. and Klabunde, K. J., " Synthesis, isolation, and chemical reactivity studies of nanocrystalline zinc oxide," *Langmuir*, 16, 3764 (2000).
51. Jo, G., Hong, W.K., Sohn, J.J., Jo, M., Shin, J., Welland, M.E., Hwang, H., Gecker, K.E. and Lee, T., " Hybrid complementary logic circuits of one dimensional Nanomaterials with adjustment of operation voltage," *Adv. Mater.*, 21, 2156 (2009).
52. Kumari ,L., and Li,W.Z., "Synthesis, structure and optical properties of zinc oxide hexagonal microprisms," *Cryst. Res. Technol.* 45, 311 – 315 (2010).

53. Rajendran, R., Balakumar, C., Mohammed Ahammed, A., Jayakumar, "Use of zinc oxide nano particles for production of antimicrobial textiles, "J. Engineering, Science and Technology, 2, 202-208, (2010).
54. Khan, K., Pratima, R., Solanki., Ajeet Kaushik., and Ansar Anees A., "Nanostructured zinc oxide platform for cholesterol sensor " Appl. Phys. Lett. 94, 143901 (2009).
55. Singh, A.K., Viswanath, V., and Janu, V.C., "Synthesis, effect of capping agents, structural, optical and photoluminescence properties of ZnO nanoparticles," J.Luminescence, 129, 874-878 (2009).
56. Ferrier, J, Xue. , Zhaohui, Li, Xuxu Wang, and Xianzhi Fu., " Studies on nanocrystalline (Sr,Pb)TiO<sub>3</sub> solid solutions prepared via a facile self-propagating combustion method" J. Physics and Chemistry of Solids , 68, 2326-2331 (2007).
57. Glogauer .M and Ferrier J. "A new method for application of force to cells via ferric oxide beads" J.Biomedical and Life Sciences , 435, 1432 (1997).
58. Ajay Kumar Gupta and Mona Gupta "Synthesis and surface engineering of iron oxide nanoparticles for biomedical applications " J. Biomaterials 26, 4021 (June 2005).
59. The World Health Organization, <http://www.who.int> 2003.
60. E. E. Calle, C. Rodriguez, K. Walker-Thurmond, M. J. Thun, N. Engl. J. Med. 348, 1625–1638, (2003).
61. Scheen, A. J., Drugs 63, 1165–1184, (2003).
62. Greenberger, N.J. , Toskes, P.P. , Harrison's Principles of Internal Medicine, vol.2, 12th ed., McGraw-Hill, New York, 1991, p. 1369.

63. Ramasubbu, N., Rangunath, C., Mishra, P.J., "Probing the role of mobile loop in substrate binding and enzyme activity of human salivary amylase," J. Mol. Biol. 5, 1061–1076 (2003).
64. Calle, E. E., Rodriguez, C., Walker-Thurmond, K., Thun, M. J., Engl. N. , J. Med. 348, 1625–1638 (2003).
65. Eichler, H. G., Korn, A., Gasic, S., Pirson, W., Businger, J., Diabetologia 26, 278–281(1984).
66. Scheen, A. J., Drugs 63, 933–951(2003).
67. G. W. Bo-Linn, C. A. Santa Ana, S. G. Morawski, and J. S. Fordtran, N.Engl. J. Med. 307, 1413 (1982).
68. Lyklema J. "*Fundamentals of Interface and Colloid Science: 1*" Academic Press (2000).
69. Wu' L., Tok' A.I.Y., Boey F.Y.C., Zeng, X.T., and Zhang, X.H., "Surface modification of ZnO nanocrystals" J.Applied Surface Science, 253, 5473-5479 (2007).